Table 2. Summary of Mutation Frequencies Detected by Using Deep Sequencing for NA808- or Telaprevir-Treated Replicon Cells

Drug	Treatment	Mutation	Region	Frequency (%)
Telaprevir	IC_{50}×6, 14 passages	V36A	NS3	18.1
		T54V	NS3	26.9
		A156T	NS3	12.9
		Q181H	NS5A	25.2
		P223S	NS5A	23.3
		S417P	NS5A	15.8
NA808	IC_{50}×6, 14 passages	Not detected		

Nucleotide sequences based on deep sequencing of NS3 to NS5B region from NA808- or telaprevir-treated replicon cells are compared with untreated controls, and amino acid mutations are shown.

intravenously with or without subcutaneous injection of PEG-IFN for 14 days. In mice infected with HCV genotype 1a, the combination therapy of NA808 with PEG-IFN led to a rapid decrease in serum HCV-RNA of about 4-log within 10 days (Figure 3*A*), and monotherapy with NA808 and PEG-IFN achieved about a 2-log and 1-log decrease, respectively (Figure 4*A*). The levels of serum HCV-RNA were also significantly reduced in genotype 2a- and 4a–infected chimeric mice that received the combination treatment (Figure 3*A*). Although sensitivities to the combination treatment varied according to HCV genotype (1a, 2a, or 4a), the serum HCV-RNA level eventually fell below the level of detection in all mice treated with the combination of NA808 and PEG-IFN (Figure 3*A*); this result was consistent with the significant reductions in hepatic HCV-RNA levels at day 14 (Figure 3*B*).

To determine if NA808 has a synergic effect with DAAs, we examined combination treatment with NS5B nucleoside inhibitor, RO-9187,[13] NS5B polymerase nonnucleoside inhibitor, HCV-796, or NS3/4A protease inhibitor, telaprevir, in HCV genotype 1a- or 1b-infected chimeric mice. Oral administration of once-daily 1000 mg/kg RO-9187, 100 mg/kg HCV-796, or 400 mg/kg telaprevir had only very limited effects or no apparent effects on serum HCV-RNA levels during the 14 days of treatment (Figure 4*B*, *C*, and *D*). However, the combination therapy of NA808 with RO-9187, HCV-796, or telaprevir led to decreases in serum HCV-RNA levels of about 2.6-log, 3.5-log, and 2.5-log, respectively, within 14 days (Figure 4*B*, *C*, and *D*); these reductions were all in excess of viral load reductions achieved by treatment with NA808 (5 mg/kg) alone. After 28 days of combination treatment with NA808 and telaprevir, serum HCV-RNA levels were reduced by 10^4-fold (data not shown). These data suggest that NA808 has synergistic antiviral effects with HCV enzyme-targeted drugs in vivo, regardless of the targeted enzyme. The combination therapy of NA808 with telaprevir and HCV-796 resulted in up to a 4.7-log reduction of serum HCV-RNA within 14 days (Figure 4*D*). At the end of the treatment, hepatic HCV-RNA levels were also reduced, correlating with the reduction of serum HCV-RNA (Figure 4*E*).

Pharmacokinetics Data of Chimeric Mice Treated With NA808

We measured the plasma concentration of NA808 in humanized-liver mice at 24 hours after 14 days of treatment. The plasma concentrations of NA808 at trough level were 0.510 ± 0.517 nmol/L (1.5 mg/kg), 0.446 ± 0.163 nmol/L (3 mg/kg), and 1.44 ± 1.07 nmol/L (5 mg/kg), respectively (Table 3). Obvious toxicological findings in general conditions were not observed at any doses. We selected 1.4 nmol/L as an effective trough level of NA808 in vivo.

Discussion

The current treatment regimen for HCV infection is combination therapy with PEG-IFN and RBV; however, this combination therapy has limited efficacy and is not well tolerated in many patients due to its systemic side-effect profile.[3,4] Although the HCV NS3/4A protease inhibitors telaprevir and SCH503034 (boceprevir) have been recently approved for the treatment of chronic HCV

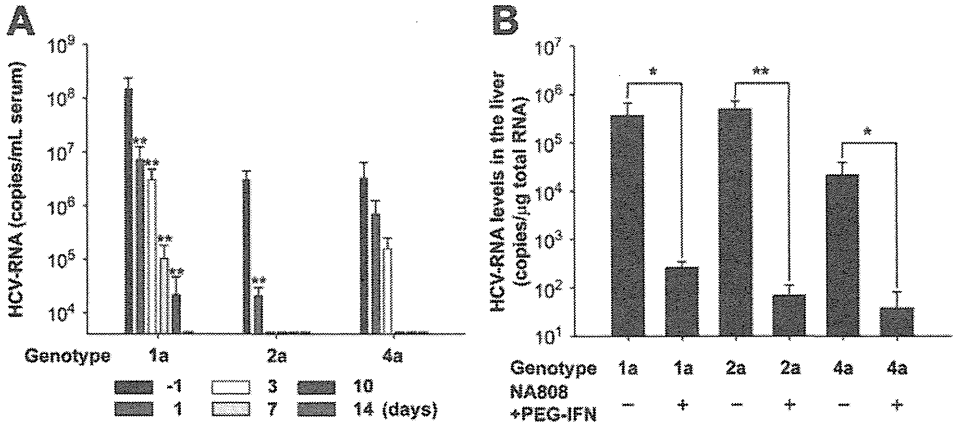

Figure 3. Antiviral effect of combination treatment of NA808 with PEG-IFN on HCV-infected chimeric mice. (*A*) Time course of serum HCV-RNA levels in chimeric mice infected with genotype 1a, 2a, or 4a and treated with a combination of NA808 (5 mg/kg/d, intravenously) and PEG-IFN (30 μg/kg/twice weekly, subcutaneously). HCV-RNA levels one day before administration are shown in *black bars*. (*B*) HCV-RNA levels in the liver 14 days after the initiation of combination therapy with NA808 and PEG-IFN. Error bars = SD. **P* < .05; ***P* < .01.

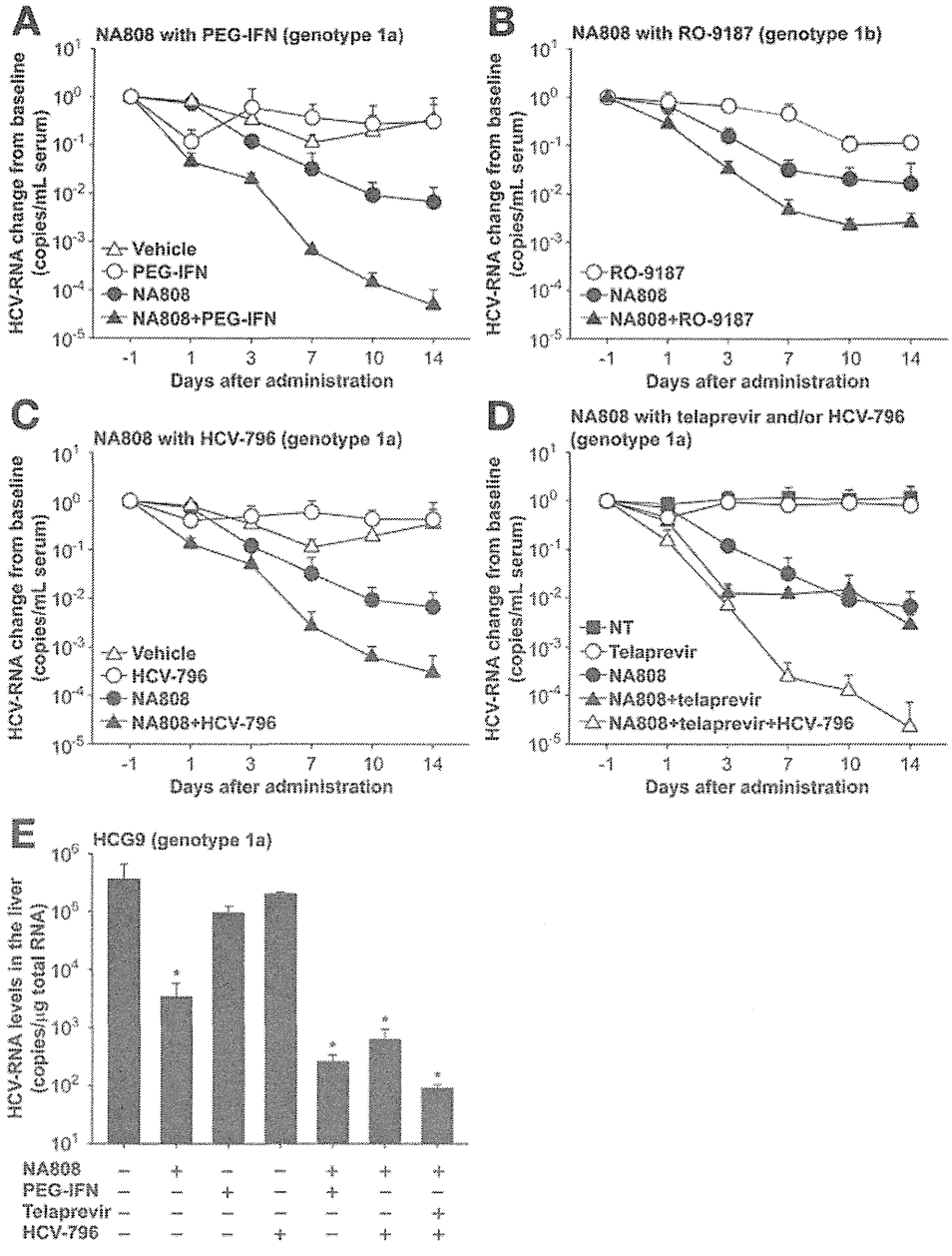

Figure 4. Combination treatment of NA808 with PEG-IFN or direct-acting antiviral agents exhibits robust anti-HCV activity in chimeric mice with humanized liver. (*A–D*) Median change from baseline of serum HCV-RNA over the 14-day monotherapy or combination therapy of NA808 (5 mg/kg/d, intravenously) with PEG-IFN (*A*: 30 μg/kg/twice weekly, subcutaneously), RO-9187 (*B*: 1000 mg/kg/d, orally), HCV-796 (*C*: 100 mg/kg/d, orally), or telaprevir (400 mg/kg/d, orally) and/or HCV-796 (*D*). (*E*) HCV-RNA levels in livers of HCG9-infected chimeric mice at the end of each treatment. Error bars = SD. (*$P < .05$).

infection, these compounds need to be combined with the current standard of care.[5] Therefore, the ultimate goal of developing a therapy for chronic hepatitis C is likely to combine HCV enzyme-targeting agents without the use of IFN or RBV. Currently, combination therapies of DAAs, such as NS3/4 serine protease inhibitors, NS5B RNA-dependent RNA polymerase inhibitors, and NS5A inhibitors, are being tested in clinical trials; however, the emergence of resistance mutations limits the efficacy of these therapies.[8,9] In addition, the antiviral activities of DAAs are reduced for certain HCV genotypes.[11] Additional antiviral agents with high barriers to resistance and potent antiviral activities against a wide variety of HCV genotypes are necessary to establish robust and effective antiviral combination therapies without the use of IFN or RBV. The infection and replication process of HCV can use not only NS3, NS4, and NS5 proteins, but also several known and unknown host protein factors. Drugs that target host protein factors could provide therapies against HCV with a high barrier to resistance.

Table 3. Plasma Concentration of NA808 in Humanized-Liver Mice at 24 Hours After Last Dosing

Dose	Concentration (nmol/L)[a]
1.5 mg/kg	0.510 ± 0.517
3.0 mg/kg	0.446 ± 0.163
5.0 mg/kg	1.44 ± 1.07

[a]Data are indicated as mean ± SD.

In the present study, we evaluated the anti-HCV activity of NA808, a novel host SPT inhibitor in vitro and in vivo. The inhibitory activity of NA808 is attributed to the inhibition of the cellular enzyme SPT, which is necessary for viral replication. The mode of action of NA255, a lead compound of NA808, is the disruption of the scaffold where the HCV replication complex forms on host cellular lipid rafts.[12] NA808 potently inhibits the de novo biosynthesis of cellular sphingolipids, such as ceramide and sphingomyelin, in a dose-dependent manner (Supplementary Figure 1*B*). We have recently reported that NA808 influences sphingolipid metabolism in host cells along with its biosynthesis and that sphingomyelin, a type of sphingolipid, plays a multifaceted role in the HCV life cycle.[18] Additionally, the alteration of sphingolipid metabolism contributes to virion maturation and infectivity in the JFH-1 culture system.[19] These results suggest that NA808 affects many phases of the life cycle, including entry, replication, and maturation. It seems that these diverse working points in the HCV life cycle along with the differentials of the target site could be a reason for the enhanced anti-HCV activity of combination treatment with NA808 and DAAs.

Myriocin, another SPT inhibitor, strongly reduces the expression of hemagglutinin and neuraminidase of influenza virus glycoproteins and inhibits the release of virus particles from infected cells.[20] The mechanism of inhibition involves the sphingomyelin biosynthetic pathway, which plays a critical role in the generation of influenza virus particles. In another report, Miller et al found that ebola virus particles strongly associate with the sphingomyelin-rich regions of the cell membrane and that depletion of sphingomyelin reduces ebola virus infection.[21] Lipid rafts, sphingolipid-enriched membrane microdomains, are involved in the entry, assembly, and budding of various types of viruses other than HCV, including several viruses with a serious public health concern. SPT inhibitors, such as NA808, have the potential to affect the life cycle of the other families of viruses and provide therapeutic options for these difficult-to-treat viral infections via the inhibition of sphingolipid biosynthesis and modification of its metabolism, as described here.

Based on the mechanism of action, NA808 could be anticipated to have antiviral activity against a wide variety of HCV genotypes as compared with DAAs. To estimate the effects of NA808 in DAA combination therapy without the use of IFN or RBV, a combinatorial treatment with NA808 and NS5B polymerase inhibitors and/or NS3/4A protease inhibitors was evaluated in chimeric mice with humanized liver infected with HCV. Both non-nucleoside inhibitors and nucleoside inhibitors of NS5B are currently being tested in clinical trials, and the most advanced protease inhibitors, such as telaprevir, are linear compounds and are currently on the market; several macrocyclic compounds are being tested in clinical trials.[11,22–25] Monotherapy with the non-nucleoside polymerase inhibitor, HCV-796, showed less than a 0.5 $\log_{10}$ reduction of serum HCV RNA levels, while a combined treatment with NA808 reduced the HCV titer by 1000-fold from the initial serum levels. This effect was higher than the effect of NA808 alone and higher than the sum of NA808 and HCV-796 monotherapy effects, suggesting synergistic antiviral efficacy. A similar effect was observed by combination of NA808 with nucleoside polymerase inhibitor, RO-9187, as shown in Figure 4*B*. The maximum reductions in HCV RNA are mediated by triple combinatorial treatment and the significant in vivo anti-HCV activity with combination treatment is also observed when NA808 is combined with PEG-IFN. These observations suggest that NA808 may have synergistic antiviral activity with various classes of anti-HCV agents, regardless of their inhibition mechanism, due to the unique host enzyme-targeted mechanism of action. In addition, NA808 could be expected to show a higher barrier to the development of resistant clones. Deep-sequencing analysis showed no evidence for the development of NA808 resistance after 14 passages in HCV replicon cells, while telaprevir treatment resulted in the selection of known protease resistance mutations (V36A, T54V, and A156T) (Table 2). The full-genome sequence of HCV obtained at day 14 from HCV-infected humanized-liver mice treated with NA808 for 14 days also showed no evidence for the selection of resistance mutations, consistent with the viral load kinetics (Figure 2B).

Host enzyme inhibition might be associated with mechanism-related toxicities or side effects. Although more thorough analyses of toxicity with NA808 are warranted, NA808 did not affect host cell viability in vitro under the assay conditions used (Supplementary Figure 1*A*), and it was well-tolerated in vivo at the efficacious dose used. The effective plasma concentration of NA808 at trough level was approximately 1.4 nmol/L (Table 3), around 100 times lower than rats that received 40 mg/kg NA808 at 24 hours after injection (data not shown). No NA808-related changes, including abnormalities of general conditions, body weight decreases, and macroscopic or microscopic changes were observed at this high dose in rats. Homozygous knockout mice for sptlc1 and sptlc2, subunits of SPT, were embryonic lethal, and heterozygous mice showed no phenotype.[26] Mice with conditional sptlc2 knockout showed necrotic lesions in gastrointestinal cells.[27] The highly selective distribution of NA808 to the liver can contribute to limit potential systemic toxicities associated with SPT inhibition by NA808.[28]

In conclusion, NA808 mediates potent anti-HCV activities in a variety of genotypes with an apparent high barrier to resistance. Synergistic effects with PEG-IFN, HCV protease, and/or polymerase inhibitors are observed in chimeric mice with humanized liver infected with HCV. These findings suggest that NA808 has potential as a novel host-targeted drug in the treatment of HCV infection. NA808 is considered a promising candidate for DAA combination treatment without the use of IFN or RBV to prevent the development of drug resistance and effectively inhibit a wide spectrum of HCV genotypes.

Supplementary Material

Note: To access the supplementary material accompanying this article, visit the online version of *Gastroenterology* at www.gastrojournal.org, and at http://dx.doi.org/10.1053/j.gastro.2013.06.012.

References

1. Wasley A, Alter MJ. Epidemiology of hepatitis C: geographic differences and temporal trends. Semin Liver Dis 2000;20:1-16.
2. Alter MJ, Kruszon-Moran D, Nainan OV, et al. The prevalence of hepatitis C virus infection in the United States, 1988 through 1994. N Engl J Med 1999;341:556-562.
3. Fried MW, Shiffman ML, Reddy KR, et al. Peginterferon alfa-2a plus ribavirin for chronic hepatitis C virus infection. N Engl J Med 2002; 347:975-982.
4. Manns MP, McHutchison JG, Gordon SC, et al. Peginterferon alfa-2b plus ribavirin compared with interferon alfa-2b plus ribavirin for initial treatment of chronic hepatitis C: a randomised trial. Lancet 2001;358:958-965.
5. **Hezode C**, **Forestier N**, Dusheiko G, et al. Telaprevir and peginterferon with or without ribavirin for chronic HCV infection. N Engl J Med 2009;360:1839-1850.
6. Kwo P, Lawitz J, McCone J, et al. 44th Annual Meeting of the European Association for the Study of the Liver, Copenhagen, Denmark, 22 to 26 April 2009, abstract 4.
7. Sarrazin C, Zeuzem S. Resistance to direct antiviral agents in patients with hepatitis C virus infection. Gastroenterology 2010;138:447-462.
8. Pawlotsky JM. Treatment failure and resistance with direct-acting antiviral drugs against hepatitis C virus. Hepatology 2011;53:1742-1751.
9. Zeuzem S, Buggisch P, Agarwal K, et al. The protease inhibitor GS-9256 and non-nucleoside polymerase inhibitor tegobuvir alone, with RBV or peginterferon plus RBV in hepatitis C. Hepatology 2012; 55:749-758.
10. Gane EJ, Roberts SK, Stedman CA, et al. Oral combination therapy with a nucleoside polymerase inhibitor (RG7128) and danoprevir for chronic hepatitis C genotype 1 infection (INFORM-1): a randomised, double-blind, placebo-controlled, dose-escalation trial. Lancet 2010; 376:1467-1475.
11. Gottwein JM, Scheel TK, Jensen TJ, et al. Differential efficacy of protease inhibitors against HCV genotypes 2a, 3a, 5a, and 6a NS3/4A protease recombinant viruses. Gastroenterology 2011;141: 1067-1079.
12. Sakamoto H, Okamoto K, Aoki M, et al. Host sphingolipid biosynthesis as a target for hepatitis C virus therapy. Nat Chem Biol 2005; 1:333-337.
13. Klumpp K, Kalayanov G, Ma H, et al. 2'-deoxy-4'-azido nucleoside analogs are highly potent inhibitors of hepatitis C virus replication despite the lack of 2'-alpha-hydroxyl groups. J Biol Chem 2008; 283:2167-2175.
14. Watanabe T, Sudoh M, Miyagishi M, et al. Intracellular-diced dsRNA has enhanced efficacy for silencing HCV RNA and overcomes variation in the viral genotype. Gene Ther 2006;13:883-892.
15. Takeuchi T, Katsume A, Tanaka T, et al. Real-time detection system for quantification of hepatitis C virus genome. Gastroenterology 1999;116:636-642.
16. Halfon P, Lacarnini S. Hepatitis C virus resistance to protease inhibitors. J Hepatol 2011;55:192-206.
17. **Inoue K**, **Umehara T**, Ruegg UT, et al. Evaluation of a cyclophilin inhibitor in hepatitis C virus-infected chimeric mice in vivo. Hepatology 2007;45:921-928.
18. Hirata Y, Ikeda K, Sudoh M, et al. Self-enhancement of hepatitis C virus replication by promotion of specific sphingolipid biosynthesis. PLoS Pathog 2012;8:e100286.
19. Aizaki H, Morikawa K, Fukasawa M, et al. Critical role of virion-associated cholesterol and sphingomyelin in hepatitis C virus infection. J Virol 2008;82:5715-5724.
20. Tafesse FG, Sanyal S, Ashour J, et al. Intact sphingomyelin biosynthetic pathway is essential for intracellular transport of influenza virus glycoproteins. Proc Natl Acad Sci U S A 2013; 110:6406-6411.
21. Miller ME, Adhikary S, Kolokoltsov AA, et al. Ebolavirus requires acid sphingomyelinase activity and plasma membrane sphingomyelin for infection. J Virol 2012;86:7473-7483.
22. Villano SA, Raible D, Harper D, et al. Antiviral activity of the non-nucleoside polymerase inhibitor, HCV-796, in combination with pegylated interferon alfa-2b in treatment-naive patients with chronic HCV. J Hepatol 2007;46:S24.
23. Shi ST, Herlihy KJ, Graham JP, et al. Preclinical characterization of PF-00868554, a potent nonnucleoside inhibitor of the hepatitis C virus RNA-dependent RNA polymerase. Antimicrob Agents Chemother 2009;53:2544-2552.
24. Le Pogam S, Seshaadri A, Ewing A, et al. RG7128 alone or in combination with pegylated interferon-alpha 2a and ribavirin prevents hepatitis C virus (HCV) replication and selection of resistant variants in HCV-infected patients. J Infect Dis 2010;202: 1510-1519.
25. Lam AM, Murakami E, Espiritu C, et al. PSI-7851, a pronucleotide of beta-D-2'-deoxy-2'-fluoro- 2'-C-methyluridine monophosphate: a potent and pan-genotype inhibitor of hepatitis C virus replication. Antimicrob Agents Chemother 2010;54:3187-3196.
26. Hojjati MR, Li Z, Jiang XC, et al. Serine palmitoyl-CoA transferase (SPT) deficiency and sphingolipid levels in mice. Biochim Biophys Acta 2005;1737:44-51.
27. Ohta E, Ohira T, Matsue K, et al. Analysis of development of lesions in mice with serine palmitoyltransferase (SPT) deficiency -Sptlc2 conditional knockout mice-. Exp Anim 2009;58:515-524.
28. Ozeki K, Okano K, Ohminato N, et al. The mechanism of the liver specific distribution of NA808, a first-in-class serine palmitoyltransferase inhibitor, mediated by organic anion transporter 1B1-multidrug resistance associated protein 2. Hepatology 2011; 54:550A.

Author names in bold designate shared co-first authorship.

Received June 16, 2012. Accepted June 10, 2013.

Reprint requests

Address requests for reprints to: Michinori Kohara, PhD, Department of Microbiology and Cell Biology, Tokyo Metropolitan Institute of Medical Science, 2-1-6 Kamikitazawa, Setagaya-ku, Tokyo 156-8506, Japan. e-mail: kohara-mc@igakuken.or.jp; fax: +81 3 5316 3137.

Acknowledgments

The authors would like to thank Yoshimi Tobita and Hiroshi Yokomichi for their technical assistance.

Conflicts of interest

The authors disclose the following: A. Katsume, K. Okamoto, Y. Ohmori, S. Fujiwara, T. Tsukuda, Y. Aoki, and M. Sudoh are employees of Chugai Pharmaceutical Co., Ltd. I. Kusanagi is an employee of Chugai Research Institute for Medical Science Inc. K. Klumpp is an employee of F. Hoffmann-La Roche Inc. The remaining authors disclose no conflicts.

Funding

This study was supported in part by a grant from the Ministry of Education, Culture, Sports, Science (213901457) and Technology of Japan and a grant from the Ministry of Health, Labour and Welfare of Japan.

Hindawi Publishing Corporation
International Journal of Hepatology
Volume 2013, Article ID 249535, 7 pages
http://dx.doi.org/10.1155/2013/249535

Hindawi

Research Article

Demonstration of Hepatitis C Virus RNA with *In Situ* Hybridization Employing a Locked Nucleic Acid Probe in Humanized Liver of Infected Chimeric Mice and in Needle-Biopsied Human Liver

Kazuya Shiogama,[1] Ken-ichi Inada,[1] Michinori Kohara,[2] Hidemi Teramoto,[3] Yasuyoshi Mizutani,[1] Takanori Onouchi,[1] and Yutaka Tsutsumi[1]

[1] *Department of Pathology, Fujita Health University School of Medicine, Toyoake, Aichi 470-1192, Japan*
[2] *Department of Microbiology and Cell Biology, Tokyo Metropolitan Institute of Medical Science, Tokyo 156-8506, Japan*
[3] *Department of Internal Medicine, Kojin Hospital, Nagoya 463-8530, Japan*

Correspondence should be addressed to Yutaka Tsutsumi; tsutsumi@fujita-hu.ac.jp

Received 30 December 2012; Revised 21 May 2013; Accepted 23 May 2013

Academic Editor: Hervé Lerat

Background. *In situ* hybridization (ISH) with high sensitivity has been requested to demonstrate hepatitis C virus (HCV) RNA in formalin-fixed, paraffin-embedded (FFPE) sections of the liver. *Methods.* ISH employing a locked-nucleic-acid- (LNA-)modified oligonucleotide probe and biotin-free catalyzed signal amplification system (CSAII) was applied to HCV-RNA detection in the liver tissue. Nested reverse-transcription polymerase chain reaction (RT-PCR) was performed for HCV genotyping using total RNA extracted from FFPE sections. The target tissues included FFPE tissue sections of humanized livers in HCV-infected chimeric mice (HCV genotypes 1a, 1b, and 2a and noninfected) and of needle-biopsied livers from HCV-infected patients. *Results.* HCV-RNA was demonstrated with the ISH technique in HCV-infected liver tissues from both chimeric mice and 9 (82%) of 11 patients with HCV infection. The HCV signals were sensitive to RNase. Nested RT-PCR confirmed the genotype in 8 (73%) of 11 livers (type 1b: 6 lesions and type 2a: 2 lesions). HCV-RNA was not identified in chronic hepatitis B lesions, fatty liver, autoimmune hepatitis, and hepatocellular carcinoma. *Conclusion.* ISH using the LNA-modified oligonucleotide probe and CSAII was applicable to detecting HCV-RNA in routinely prepared FFPE liver specimens.

1. Introduction

Hepatitis C virus (HCV) is a single-stranded RNA virus, a member of the Flaviviridae family. Since the first identification of the HCV genome by Choo et al. [1], HCV study has progressed mainly in the field of HCV functional analysis and therapeutic implications. Because of low viral levels in the serum, the diagnosis of HCV infection has been made with a branched chain DNA signal amplification assay and reverse-transcription polymerase chain reaction (RT-PCR) [2–4]. The sensitivity of HCV detection in the serum thus became reproducible and clinically relevant.

Pathologists are often requested to detect viral pathogens within the routinely prepared biopsy tissue samples, and therefore simple and reliable histochemical techniques are needed. Techniques for visualizing HCV localization within diseased hepatocytes have also been developed. Reports have described the detection of HCV in human liver tissue by using immunohistochemistry and *in situ* hybridization (ISH) [4–14], as well as by *in situ* RT-PCR [4, 6, 15–20]. At the moment, HCV detection with immunohistochemistry and ISH is not yet reproducible enough, we believe. *In situ* RT-PCR may demonstrate highly sensitive signals, but with concomitant increase of false positivity. Reliable histochemical techniques for detecting HCV in formalin-fixed, paraffin-embedded (FFPE) liver tissues are needed, particularly for routine diagnostic purpose.

In the present study, we established an ISH technique using a locked nucleic acid (LNA) probe and biotin-free tyramide amplification system (CSAII) for detecting HCV-RNA in FFPE tissue sections of the liver.

2. Materials and Methods

2.1. Samples. As positive controls, we sampled the humanized liver of HCV-infected chimeric mice [21, 22], and FFPE tissue sections were prepared. The chimeric mice were maintained by M. Kohara, Department of Microbiology and Cell Biology, Tokyo Metropolitan Institute of Medical Science, Tokyo. A total of 13 humanized liver specimens from HCV-infected chimeric mice were used (noninfected 3, genotype 1a-infected 3, genotype 1b-infected 4, and genotype 2a-infected 3).

A total of 11 needle biopsy liver specimens of chronic hepatitis C were culled from the computer file at the Diagnostic Pathology Division of Fujita Health University Hospital, Toyoake, Japan, and FFPE sections were cut. Needle biopsy specimens of hepatitis-B-virus- (HBV-)infected chronic hepatitis, virus-negative fatty liver and autoimmune hepatitis ($n = 1$, resp.), as well as two surgically removed HCC lesions caused by HCV or HBV infection, were also examined. The nonneoplastic part of the liver tissue (chronic hepatitis B) in the HBV-related HCC case was also evaluated. Nonneoplastic liver tissue was scarcely included in the HCV-related HCC case. Hematoxylin and eosin (HE) staining was performed for demonstrating histological features. The activity of inflammation and the degree of fibrosis were evaluated according to the New Inuyama Classification (1996) [23]. Serum HCV-RNA levels in the patients were measured using an RT-PCR assay, the Amplicor HCV Monitor Assay (Roche Diagnostics), and serum HCV subtypes were determined with nested RT-PCR (Roche Diagnostics).

2.2. LNA-Modified Oligonucleotide Probe. The sequence of an HCV-common probe was designed according to the previous description [15]. The target was within the HCV 5′-untranslated region (HCV-5′UTR), which is a highly conserved portion in the HCV genome. An LNA-modified oligonucleotide probe labeled with digoxygenin at the 3′-end was prepared in Gene Design Inc., Ibaraki, Osaka, Japan. The nucleotide sequence of the 45-mer probe was 5′-ALtTTLgGGLcGTLgCCLcCCLgCGLaGALcTGLcTALg-CCLgAGLtAGLtGTLtGGLgT-3′, in which La, Lt, Lc, and Lg represent LNA monomers corresponding to the bases A, T, C, and G, respectively.

2.3. ISH. FFPE sections were dewaxed in xylene and rehydrated in graded ethanol. Endogenous peroxidase activity was quenched with 0.3% hydrogen peroxide in methanol for 60 minutes at room temperature (RT). After rinsing thrice in diethyl-pyrocarbonate- (DEPC-)treated water, sections were digested with 40 μg/mL proteinase K (Roche Diagnostics, Tokyo, Japan) at 37°C for 15 minutes, washed thrice in DEPC-treated water, submerged in 95% ethanol for 1 minute, and air-dried completely. Then, sections were heat-treated for 5 minutes at 95°C on a hot plate and hybridized with 0.01 μmol/L LNA-modified oligonucleotide probe diluted with *in situ* Hybridization Buffer (Enzo Life Science, Bulter Pike, PA, USA) in an incubation chamber overnight at 37°C. After rinsing in 1x saline sodium citrate (SSC) for 30 minutes at 50°C, sections were rinsed twice in 50 mM Tris-HCl-buffered saline (TBS), pH 7.6, at RT. A horseradish-peroxidase-labeled antidigoxygenin antibody (Roche Diagnostics) diluted at 1 : 100 with 1% bovine serum albumin in TBS was applied for 60 minutes at RT. For amplifying signals, fluorescein-isothiocyanate- (FITC-)conjugated tyramide enclosed in CSAII (Dako, Glostrup, Denmark) was applied to the sections for 15 minutes at RT. Finally, a horseradish-peroxidase-labeled anti-FITC antibody equipped in the CSAII kit was reacted for 30 minutes at RT. Reaction products were visualized in 50 mM Tris-HCl buffer, pH 7.6, containing 20 mg/dL diaminobenzidine tetrahydrochloride and 0.006% hydrogen peroxidase. The nuclei were lightly counterstained with Mayer's hematoxylin.

In order to verify the specificity of the ISH technique for HCV-RNA detection, we carried out the treatment with DNase and RNase before the hybridization with the LNA probe on consecutive sections. Namely, either 10 IU/mL DNase I (Wako, Osaka, Japan) or 100 μg/mL RNase (Sigma-Aldrich, St. Louis, MO, USA) was incubated for 30 minutes at 37°C.

2.4. Immunostaining Using a Human Specific Cytokeratin 8/18 (CK8/18) Antibody. In order to distinguish mouse hepatocytes from chimeric human hepatocytes in HCV-infected chimeric mice, we utilized a human-specific CK8/18 monoclonal antibody (clone: NCL 5D3, MP Biochemicals, Santa Ana, CA, USA). After blocking endogenous peroxidase activity, hydrated heat-assisted epitope retrieval was employed using a pressure pan cooker (Delicio 6L, T-FAL, Clichy, France) for 10 minutes. Preliminary study revealed that as a soaking solution, 1 mM ethylenediamine tetraacetic acid solution, pH 8.0, was optimal to retrieve the antigenicity. After pressure cooking, sections were left for 30 minutes at RT for cooling. In order for avoiding nonspecific signals in mouse hepatocytes, a Mouse Stain kit (Nichirei Bioscience, Tokyo) was applied before and after the primary antibody incubation. The human-specific CK8/18 monoclonal antibody at a 1 : 100 dilution was incubated overnight at RT. After rinsing in 10 mM phosphate-buffered saline (PBS), pH 7.2, the sections were reacted with a secondary polymer reagent, Novolink (Novocastra, Newcastle, UK). Reaction products were visualized in the diaminobenzidine-hydrogen peroxide solution. Nuclear counterstaining with hematoxylin followed.

2.5. HCV Genotyping by Nested RT-PCR. Five slices of 5 μm thickness sections were collected in Eppendorf tubes. Total RNA was extracted from dewaxed sections using RecoverAll Total Nucleic Acid Isolation kit (Applied Biosytems, Austin, TX, USA), according to the manufacturer's protocol, and stored at −80°C until use. Nested RT-PCR for HCV genotyping was performed, as described previously [24].

Table 1: HCV-RNA demonstration with LNA-based ISH and nested RT-PCR in FFPE human liver tissues.

Patient	Biopsy or surgery	Diagnosis New Inuyama Classification	Serum		FFPE liver tissue		
			HCV-RNA (KIU/mL)	Nested RT-PCR	Nested RT-PCR	ISH	
Case 1	B	Chronic hepatitis C, A2F2	$5{,}1 \times 10^2 \leqq$	1b	1b	+	Focal/partial
Case 2	B	Chronic hepatitis C, A1F1	$2{,}8 \times 10^2$	1b	1b	+	Focal/partial
Case 3	B	Chronic hepatitis C, A2,F1	$2{,}4 \times 10^2$	2a	2a	+	Diffuse
Case 4	B	Chronic hepatitis C, A1F0	$1{,}9 \times 10^2$	2a	2a	−	
Case 5	B	Chronic hepatitis C, A1F1	$2{,}5 \times 10^2$	1b	1b	+	Focal/partial
Case 6	B	Chronic hepatitis C, A2F3	$2{,}7 \times 10^2$	1b	−	−	
Case 7	B	Chronic hepatitis C, A2F1	$2{,}2 \times 10^2$	2a	−	+	Focal/partial
Case 8	B	Chronic hepatitis C, A3F3	$5{,}1 \times 10^2$	1b	1b	+	Focal/partial
Case 9	B	Chronic hepatitis C, A2F1	$2{,}9 \times 10^2$	1b	1b	+	Diffuse
Case 10	B	Chronic hepatitis C, A2F2	$3{,}1 \times 10^2$	2a	−	+	Focal/partial
Case 11	B	Chronic hepatitis C, A2F3	$3{,}3 \times 10^2$	1b	1b	+	Diffuse
Case 12	B	Chronic hepatitis B, A3F3	Not detected	Not done	−	−	
Case 13	B	Fatty liver, A0F0	Not detected	Not done	−	−	
Case 14	B	Autoimmune hepatitis, A3F3	Not detected	Not done	−	−	
Case 15	S	Hepatitis-B-related HCC Chronic hepatitis B, A2F2	Not detected	Not done	−	− −	
Case 16	S	Hepatitis-C-related HCC	84	Not done	−	−	

New Inuyama Classification (1996).
Activity of inflammation: A1: mild, A2: moderate, and A3: severe.
Fibrosis: F0: none, F1: portal widening, F2: bridging fibrosis, and F3: bridging fibrosis with lobular distortion.

2.6. Ethical Issue. The present study was approved by the institutional ethical review board for clinical and epidemiological investigations at Fujita Health University, Toyoake. The approval number is 12-193. Written informed consent was obtained from each patient.

3. Results

3.1. HCV-RNA Localization in Humanized Liver of HCV-Infected Chimeric Mice. In HE-stained sections, mouse hepatocytes showed densely eosinophilic cytoplasm, while chimeric human hepatocytes were weakly eosinophilic with frequent deposition of fat droplets. Immunoreactivity of human CK8/18 was seen only in human hepatocytes. In all the 10 HCV-infected livers but not the livers of three HCV noninfected mice, ISH demonstrated diffuse cytoplasmic signals in the human hepatocytes. In Figure 1 employing consecutive sections, HCV-RNA was visualized with the ISH technique in human CK8/18-positive chimeric hepatocytes from chimeric mice infected HCV genotypes 1a, 1b, and 2a (in Figure 1, dotted lines encircle the mouse hepatocyte area). No signals were detected in the noninfected chimeric liver tissue. It is of note that HCV-RNA was demonstrated in the cytoplasm of almost all chimeric human hepatocytes. The positive signals remained after DNase treatment but were completely abolished after RNase treatment. Figure 2 illustrates HCV genotype 1b-infected chimeric mouse liver, showing HE histology and positive cytoplasmic signals, which were resistant to DNase but sensitive to RNase.

3.2. HCV-RNA Localization in Needle-Biopsied or Surgically Removed Human Liver Tissues. Results of the human material are summarized in Table 1. Most of the HCV-positive patients showed high levels of HCV-RNA in the serum. Exceptionally, a surgical case of HCV-related HCC showed a low level of HCV-RNA in the serum. Nested RT-PCR genotyping for HCV using total RNA extracted from FFPE sections was successful in 8 (73%) of 11 biopsied chronic hepatitis C lesions, and in all the 8 cases, the genotypes were comparable with the serum analysis. LNA-based ISH detected signals in 9 (82%) of 11 chronic hepatitis C lesions, including three showing diffuse cytoplasmic positivity, and six showing focal or partial positivity. In three nested RT-PCR negative lesions, ISH revealed negativity (1 lesion) or focal/partial positivity (2 lesions). One lesion was nested RT-PCR-positive and ISH-negative. No HCV-RNA was detected in HBV-related lesions, fatty liver, autoimmune hepatitis, and in HCC lesions. Figure 3 demonstrates representative histochemical findings. Nonspecific binding of the CSAII reagent to Kupffer cells or lymphoid cells was occasionally observed in both the HCV-infected and HCV-unrelated lesions, as arrows indicate.

4. Discussion

We showed herein that LNA-based ISH for HCV-RNA yielded clear cytoplasmic reactivity in infected hepatocytes in FFPE sections. The LNA-modified oligonucleotide probe we employed represents one of the most sensitive probes for

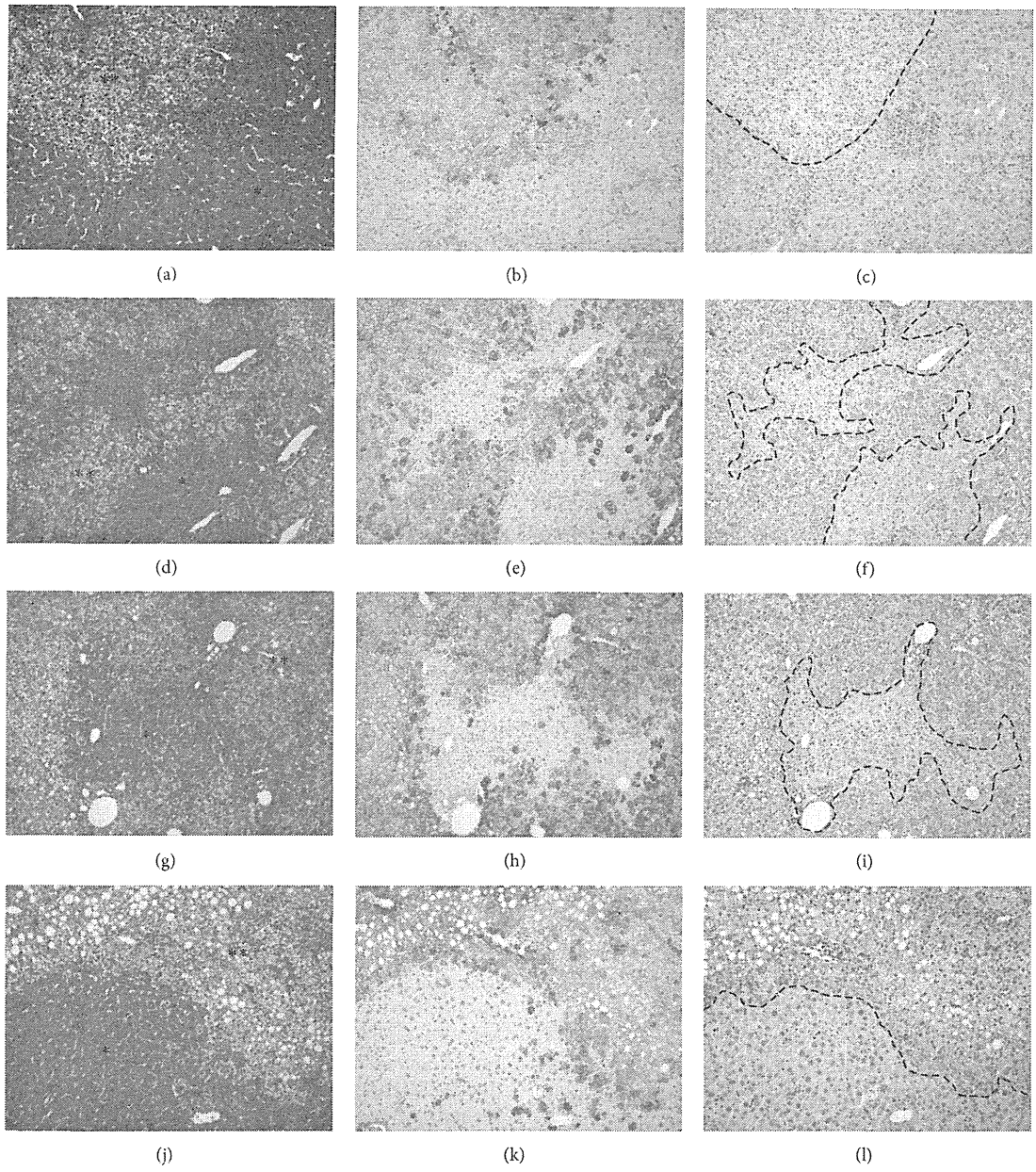

FIGURE 1: HCV-RNA localization with LNA-based ISH in the liver of chimeric mice infected with HCV of different genotypes. (a)–(c) HCV noninfected, (d)–(f) HCV genotype 1a-infected, (g)–(i) HCV genotype 1b-infected, (j)–(l) HCV genotype 2a-infected, ((a), (d), (g), (j)) HE stain, ((b), (e), (h), (k)) immunostaining for human-specific CK8/18, ((c), (f), (i), (l)) LNA-based ISH, (*) mouse hepatocytes, and (**) human hepatocytes. HCV-RNA is demonstrated diffusely in the cytoplasm of human hepatocytes in the chimeric livers. No signals are seen in the noninfected liver.

ISH [25–29]. LNA-based ISH has been applied to detecting cellular microRNA in FFPE tumor tissues [30–32]. The 45-mer LNA probe was targeted at the HCV-5′UTR containing a sequence common to the HCV subtypes. Positive signals for HCV-RNA were clearly demonstrated in HCV 1a-, 1b-, and 2a-infected humanized livers of chimeric mice. HCV-infected chimeric mice with humanized liver thus functioned as a useful model for histochemically demonstrating the HCV genome, particularly when immunostaining for human-specific CK8/18 was combined.

In needle-biopsied human liver specimens, HCV-RNA was detected in 8 of 11 HCV-infected samples with the nested RT-PCR analysis and in 9 of 11 with the ISH technique. In nested RT-PCR negative cases, ISH was negative or partially

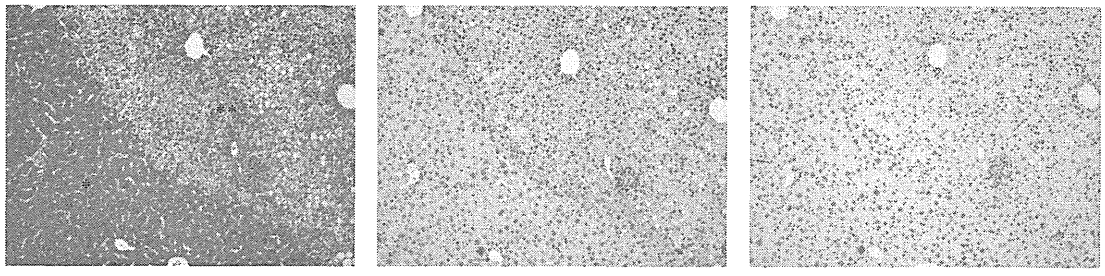

(a) (b) (c)

FIGURE 2: Confirmation of the specificity of LNA-based ISH. (a) HE stain, (b) ISH after DNase treatment, (c) ISH after RNase treatment, (*) mouse hepatocytes, and (**) human hepatocytes. The mouse hepatocytes are densely eosinophilic, while the human hepatocytes appear pale with deposition of fat droplets. HCV-RNA is observed only in the human hepatocytes in the chimeric liver infected with HCV genotype 1b. The HCV-RNA signals are resistant to DNase treatment but disappear after RNase treatment.

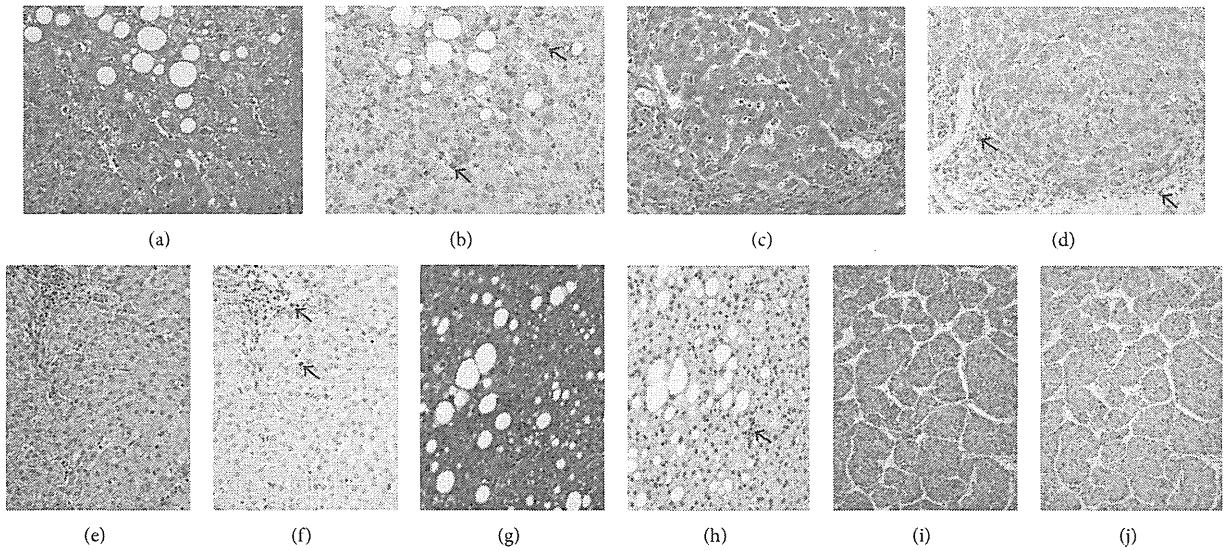

(a) (b) (c) (d)

(e) (f) (g) (h) (i) (j)

FIGURE 3: HCV-RNA localization with LNA-based ISH in FFPE biopsy or surgical specimens of the liver. ((a), (b)) Case 10 with chronic hepatitis C, ((c), (d)) case 11 with chronic hepatitis C, ((e), (f)) case 15 with chronic hepatitis B (noncancerous portion of a surgical case for HCC), ((g), (h)) case 13 with fatty liver, ((i), (j)) case 16 with surgically removed hepatitis-C-related HCC, ((a), (c), (e), (g), (i)) HE stain, and ((b), (d), (f), (h), (j)) LNA-based ISH. In HCV-infected human livers, the HCV-RNA signals are demonstrated in a focal/partial pattern (b) or in a diffuse pattern (d). Signals are not demonstrated in the hepatocytes of HBV-infected liver (f), fatty liver (h), and hepatitis-C-related HCC (j). Nonspecific binding of the reagent to Kupffer cells and lymphoid cells is occasionally observed (arrows in the panels (b), (d), (f), and (h)).

positive, suggesting that the detection threshold may depend on the virus load. Diffuse HCV expression pattern in the hepatocytes was already reported by Nuriya et al. [15], Liang et al. [33], and Li et al. [34].

In the present ISH study, HCV-RNA was undetectable in the hepatocytes in HBV-infected livers, nonviral liver disorders (fatty liver and autoimmune hepatitis), and in HCV-related HCC. With ISH using a digoxygenin-labeled cDNA probe, Tang et al. reported positivity in 8 (67%) of 12 HCV-related HCC [12]. It has been documented with an *in situ* RT-PCR technique that HCV-RNA decreases along with the progression from liver cirrhosis to HCC [35]. More cases of HCC need to be analyzed, in relation to the distribution of the HCV genome in cancerous lesions.

Revie and Salahuddin reviewed that HCV replicated in macrophages, B and T lymphocytes, and other nonhepatocellular components [36]. However, we judged the nonhepatocellular bindings as nonspecific reactions, primarily because of the staining in non-HCV cases. Under our present condition, nonspecific binding of the reagents, particularly CSAII, to Kupffer cells and lymphoid cells was observed. Further technical improvement is requested for reliable and reproducible HCV-RNA detection in FFPE specimens.

In conclusion, the ISH technique using the LNA-modified oligonucleotide probe and CSAII can be applied to detecting

HCV-RNA in liver biopsy specimens, the sensitivity probably being comparable to *in situ* RT-PCR. For detecting the HCV genome in routinely prepared liver biopsy specimens, our ISH sequence is relatively simple and requires no special equipment to perform. At the moment, this method seems to be suitable for demonstrating HCV genome in FFPE sections and will become a valuable tool for routine histopathological diagnosis of HCV infection using FFPE liver biopsy specimens.

Conflict of Interests

The authors have no conflict of interests.

Acknowledgments

The authors thank Mr. Yutaka Hirasawa and Ms. Satomi Ito, Division of Diagnostic Pathology, Fujita Health University Hospital, for their cooperation in culling the specimens. Professor Kentaro Yoshioka, Department of Liver, Biliary Tract and Pancreas Diseases, and Professor Atsushi Sugioka, Department of Surgery, Fujita Health University School of Medicine, Toyoake, kindly allowed the authors to use the biopsy specimens. The skillful technical assistance by Ms. Mika Maeshima and Ms. Sayaka Takeuchi, Department of Pathology, Fujita Health University School of Medicine, is also cordially acknowledged. This work was in part supported by the Research Grant-in-Aid from the Japanese Ministry of Education, Culture, Sports, Science and Technology (no. 24790367).

References

[1] Q.-L. Choo, G. Kuo, A. J. Weiner, L. R. Overby, D. W. Bradley, and M. Houghton, "Isolation of a cDNA clone derived from a blood-borne non-A, non-B viral hepatitis genome," *Science*, vol. 244, no. 4902, pp. 359–362, 1989.

[2] A. M. Majid and D. R. Gretch, "Current and future hepatitis C virus diagnostic testing: problems and advancements," *Microbes and Infection*, vol. 4, no. 12, pp. 1227–1236, 2002.

[3] L. Muratori, "*In situ* reverse transcriptase-polymerase chain reaction: an innovative tool for hepatitis C virus RNA detection and localisation, and for quantification of infected cells," *European Journal of Histochemistry*, vol. 42, no. 2, pp. 133–136, 1998.

[4] P. Komminoth, V. Adams, A. A. Long et al., "Evaluation of methods for hepatitis C virus detection in archival liver biopsies. Comparison of histology, immunohistochemistry, *in-situ* hybridization, reverse transcriptase polymerase chain reaction (RT-PCR) and *in-situ* RT-PCR," *Pathology Research and Practice*, vol. 190, no. 11, pp. 1017–1025, 1994.

[5] H. S. Carvalho, M. L. Baptista, M. A. Pinto et al., "Detection of hepatitis C virus RNA by *in situ* hybridization in paraformaldehyde fixed biopsies," *Memorias do Instituto Oswaldo Cruz*, vol. 100, no. 3, pp. 269–272, 2005.

[6] X. Qian, R. B. Guerrero, T. B. Plummer, V. F. Alves, and R. V. Lloyd, "Detection of hepatitis C virus RNA in formalin-fixed paraffin-embedded sections with digoxigenin-labeled cRNA probes," *Diagnostic Molecular Pathology*, vol. 13, no. 1, pp. 9–14, 2004.

[7] S. de Lucas, J. Bartolomé, E. Rodríguez-Iñigo et al., "Distribution of hepatitis C virus infection in liver biopsies from children and adults with chronic hepatitis C," *Journal of Medical Virology*, vol. 64, no. 1, pp. 1–5, 2001.

[8] M. Chang, A. P. Marquardt, B. L. Wood et al., "*in situ* distribution of hepatitis C virus replicative-intermediate RNA in hepatic tissue and its correlation with liver disease," *Journal of Virology*, vol. 74, no. 2, pp. 944–955, 2000.

[9] V. Agnello, G. Ábel, G. B. Knight, and E. Muchmore, "Detection of widespread hepatocyte infection in chronic hepatitis C," *Hepatology*, vol. 28, no. 2, pp. 573–584, 1998.

[10] D. Sansonno, V. Cornacchiulo, V. Racanelli, and F. Dammacco, "*In situ* simultaneous detection of hepatitis C virus RNA and hepatitis C virus-related antigens in hepatocellular carcinoma," *Cancer*, vol. 80, no. 1, pp. 22–33, 1997.

[11] S. W. Cho, S. G. Hwang, D. C. Han et al., "*In situ* detection of hepatitis C virus RNA in liver tissue using a digoxigenin-labeled probe created during a polymerase chain reaction," *Journal of Medical Virology*, vol. 48, no. 3, pp. 227–233, 1996.

[12] L. Tang, Y. Tanaka, N. Enomoto, F. Marumo, and C. Sato, "Detection of hepatitis C virus RNA in hepatocellular carcinoma by *in situ* hybridization," *Cancer*, vol. 76, no. 11, pp. 2211–2216, 1995.

[13] M. Gastaldi, A. Massacrier, R. Planells et al., "Detection by *in situ* hybridization of hepatitis C virus positive and negative RNA strands using digoxigenin-labeled cRNA probes in human liver cells," *Journal of Hepatology*, vol. 23, no. 5, pp. 509–518, 1995.

[14] Y. Tanaka, N. Enomoto, S. Kojima et al., "Detection of hepatitis C virus RNA in the liver by *in situ* hybridization," *Liver*, vol. 13, no. 4, pp. 203–208, 1993.

[15] H. Nuriya, K. Inoue, T. Tanaka et al., "Detection of hepatitis B and C viruses in almost all hepatocytes by modified PCR-based *in situ* hybridization," *Journal of Clinical Microbiology*, vol. 48, no. 11, pp. 3843–3851, 2010.

[16] A. J. Alzahrani, P. J. Vallely, and R. F. T. McMahon, "Development of a novel nested *in situ* PCR-ISH method for detection of hepatitis C virus RNA in liver tissue," *Journal of Virological Methods*, vol. 99, no. 1-2, pp. 53–61, 2002.

[17] P. Biagini, L. Benkoel, F. Dodero et al., "Hepatitis C virus RNA detection by *in situ* RT-PCR in formalin-fixed paraffin-embedded liver tissue. Comparison with serum and tissue results," *Cellular and Molecular Biology*, vol. 47, pp. OL167–OL171, 2001.

[18] D. Bettinger, C. Mougin, B. Fouqué, B. Kantelip, J. P. Miguet, and M. Lab, "Direct *in situ* reverse transcriptase-linked polymerase chain reaction with biotinylated primers for the detection of hepatitis C virus RNA in liver biopsies," *Journal of Clinical Virology*, vol. 12, no. 3, pp. 233–241, 1999.

[19] F. M. Walker, M. Dazza, M. Dauge et al., "Detection and localization by *in situ* molecular biology techniques and immunohistochemistry of hepatitis C virus in livers of chronically infected patients," *Journal of Histochemistry and Cytochemistry*, vol. 46, no. 5, pp. 653–660, 1998.

[20] G. K. K. Lau, J. W. S. Fang, P. C. Wu, G. L. Davis, and J. Y. N. Lau, "Detection of hepatitis C virus genome in formalin-fixed paraffin-embedded liver tissue by *in situ* reverse transcription polymerase chain reaction," *Journal of Medical Virology*, vol. 44, no. 4, pp. 406–409, 1994.

[21] C. Tateno, Y. Yoshizane, N. Saito et al., "Near completely humanized liver in mice shows human-type metabolic responses to drugs," *American Journal of Pathology*, vol. 165, no. 3, pp. 901–912, 2004.

[22] D. F. Mercer, D. E. Schiller, J. F. Elliott et al., "Hepatitis C virus replication in mice with chimeric human livers," *Nature Medicine*, vol. 7, no. 8, pp. 927–933, 2001.

[23] F. Ichida, "Histological grading criteria of chronic hepatitis: new Inuyama classification," in *Proceedings of the 19th Inuyama Symposium*, pp. 183–188, Chugai Igaku, 1996.

[24] K. Shiogama, H. Teramoto, Y. Morita et al., "Hepatitis C virus infection in a Japanese leprosy sanatorium for the past 67 years," *Journal of Medical Virology*, vol. 82, no. 4, pp. 556–561, 2010.

[25] L. A. Neely, S. Patel, J. Garver et al., "A single-molecule method for the quantitation of microRNA gene expression," *Nature Methods*, vol. 3, no. 1, pp. 41–46, 2006.

[26] W. P. Kloosterman, E. Wienholds, E. de Bruijn, S. Kauppinen, and R. H. A. Plasterk, "*In situ* detection of miRNAs in animal embryos using LNA-modified oligonucleotide probes," *Nature Methods*, vol. 3, no. 1, pp. 27–29, 2006.

[27] K. Kubota, A. Ohashi, H. Imachi, and H. Harada, "Improved *in situ* hybridization efficiency with locked-nucleic-acid- incorporated DNA probes," *Applied and Environmental Microbiology*, vol. 72, no. 8, pp. 5311–5317, 2006.

[28] R. Thomsen, P. S. Nielsen, and T. H. Jensen, "Dramatically improved RNA *in situ* hybridization signals using LNA-modified probes," *RNA*, vol. 11, no. 11, pp. 1745–1748, 2005.

[29] A. Válóczi, C. Hornyik, N. Varga, J. Burgyán, S. Kauppinen, and Z. Havelda, "Sensitive and specific detection of microRNAs by northern blot analysis using LNA-modified oligonucleotide probes," *Nucleic Acids Research*, vol. 32, no. 22, article e175, 2004.

[30] K. Sakurai, C. Furukawa, T. Haraguchi et al., "MicroRNAs miR-199a-5p and -3p target the Brm subunit of SWI/SNF to generate a double-negative feedback loop in a variety of human cancers," *Cancer Research*, vol. 71, no. 5, pp. 1680–1689, 2011.

[31] N. Yamamichi, R. Shimomura, K. Inada et al., "Locked nucleic acid *in situ* hybridization analysis of miR-21 expression during colorectal cancer development," *Clinical Cancer Research*, vol. 15, no. 12, pp. 4009–4016, 2009.

[32] P. T. Nelson, D. A. Baldwin, W. P. Kloosterman, S. Kauppinen, R. H. A. Plasterk, and Z. Mourelatos, "RAKE and LNA-ISH reveal microRNA expression and localization in archival human brain," *RNA*, vol. 12, no. 2, pp. 187–191, 2006.

[33] Y. Liang, T. Shilagard, S. Xiao et al., "Visualizing hepatitis C virus infections in human liver by two-photon microscopy," *Gastroenterology*, vol. 137, no. 4, pp. 1448–1458, 2009.

[34] G. Li, K. Li, A. S. Lea et al., "*In situ* hybridization for the detection of hepatitis C virus RNA in human liver tissue," *Journal of Viral Hepatitis*, vol. 20, no. 3, pp. 183–192, 2013.

[35] T. Tanaka, K. Inoue, Y. Hayashi et al., "Virological significance of low-level hepatitis B virus infection in patients with hepatitis C virus associated liver disease," *Journal of Medical Virology*, vol. 72, no. 2, pp. 223–229, 2004.

[36] D. Revie and S. Z. Salahuddin, "Human cell types important for Hepatitis C Virus replication *in vivo* and *in vitro*. Old assertions and current evidence," *Virology Journal*, vol. 8, pp. 346–370, 2011.

OPEN ACCESS Freely available online

PLOS ONE

Targeted Induction of Interferon-λ in Humanized Chimeric Mouse Liver Abrogates Hepatotropic Virus Infection

Shin-ichiro Nakagawa[1,2☯], Yuichi Hirata[1,10☯], Takeshi Kameyama[3], Yuko Tokunaga[1], Yasumasa Nishito[4], Kazuko Hirabayashi[2], Junichi Yano[2], Takahiro Ochiya[5], Chise Tateno[6], Yasuhito Tanaka[7], Masashi Mizokami[8], Kyoko Tsukiyama-Kohara[9], Kazuaki Inoue[10], Makoto Yoshiba[10], Akinori Takaoka[3], Michinori Kohara[1]*

1 Department of Microbiology and Cell Biology, Tokyo Metropolitan Institute of Medical Science, Setagaya-ku, Tokyo, Japan, **2** Discovery Research Laboratories, Nippon Shinyaku Co., Ltd., Tsukuba, Ibaraki, Japan, **3** Division of Signaling in Cancer and Immunology, Institute for Genetic Medicine, Hokkaido University, Sapporo, Hokkaido, Japan, **4** Center for Microarray Analysis, Tokyo Metropolitan Institute of Medical Science, Setagaya-ku, Tokyo, Japan, **5** Division of Molecular and Cellular Medicine, Japanese National Cancer Center Research Institute, Chuo-ku, Tokyo, Japan, **6** PhoenixBio Co., Ltd., Higashi-Hiroshima, Hiroshima, Japan, **7** Department of Virology and Liver Unit, Nagoya City University Graduate School of Medical Science, Nagoya, Aichi, Japan, **8** Research Center for Hepatitis and Immunology, International Medical Center of Japan Konodai Hospital, Ichikawa, Chiba, Japan, **9** Transboundary Animal Diseases Center, Joint Faculty of Veterinary Medicine, Kagoshima University, Kagoshima, Japan, **10** Division of Gastroenterology, Showa University Fujigaoka Hospital, Yokohama, Kanagawa, Japan

Abstract

Background & Aims: The interferon (IFN) system plays a critical role in innate antiviral response. We presume that targeted induction of IFN in human liver shows robust antiviral effects on hepatitis C virus (HCV) and hepatitis B virus (HBV).

Methods: This study used chimeric mice harboring humanized livers and infected with HCV or HBV. This mouse model permitted simultaneous analysis of immune responses by human and mouse hepatocytes in the same liver and exploration of the mechanism of antiviral effect against these viruses. Targeted expression of IFN was induced by treating the animals with a complex comprising a hepatotropic cationic liposome and a synthetic double-stranded RNA analog, pIC (LIC-pIC). Viral replication, IFN gene expression, IFN protein production, and IFN antiviral activity were analyzed (for type I, II and III IFNs) in the livers and sera of these humanized chimeric mice.

Results: Following treatment with LIC-pIC, the humanized livers of chimeric mice exhibited increased expression (at the mRNA and protein level) of human IFN-λs, resulting in strong antiviral effect on HBV and HCV. Similar increases were not seen for human IFN-α or IFN-β in these animals. Strong induction of IFN-λs by LIC-pIC occurred only in human hepatocytes, and not in mouse hepatocytes nor in human cell lines derived from other (non-hepatic) tissues. LIC-pIC-induced IFN-λ production was mediated by the immune sensor adaptor molecules mitochondrial antiviral signaling protein (MAVS) and Toll/IL-1R domain-containing adaptor molecule-1 (TICAM-1), suggesting dual recognition of LIC-pIC by both sensor adaptor pathways.

Conclusions: These findings demonstrate that the expression and function of various IFNs differ depending on the animal species and tissues under investigation. Chimeric mice harboring humanized livers demonstrate that IFN-λs play an important role in the defense against human hepatic virus infection.

Citation: Nakagawa S-i, Hirata Y, Kameyama T, Tokunaga Y, Nishito Y, et al. (2013) Targeted Induction of Interferon-λ in Humanized Chimeric Mouse Liver Abrogates Hepatotropic Virus Infection. PLoS ONE 8(3): e59611. doi:10.1371/journal.pone.0059611

Editor: Kui Li, University of Tennessee Health Science Center, United States of America

Received October 3, 2012; **Accepted** February 15, 2013; **Published** March 28, 2013

Funding: This study was supported by grants from the Ministry of Education, Culture, Sports, Science, and Technology of Japan; the Program for Promotion of Fundamental Studies in Health Science of the National Institute of Biomedical Innovation of Japan; and the Ministry of Health, Labor, and Welfare of Japan. The funders had no role in study design, data collection and analysis, decision to publish, or preparation of the manuscript.

Competing Interests: With regards to competing interest, Shin-ichiro Nakagawa, Kazuko Hirabayashi, and Junichi Yano are employees of Nippon Shinyaku Co., Ltd. Chise Tateno is an employee of PhoenixBio Co. Ltd. This does not alter the authors' adherence to all the PLOS ONE policies on sharing data and materials.

* E-mail: kohara-mc@igakuken.or.jp

☯ These authors contributed equally to this work.

Introduction

The interferon (IFN) family of cytokines are important mediators of the innate immune response and contribute to the first line of defense against viral infection. The IFNs are classified as type I (IFN-α and IFN-β), type II (IFN-γ), or type III (IFN-λ), based on receptor complex recognition and protein structure.

Innate immune responses, such as IFN induction, contribute to defenses against microbial pathogens. Pathogens are recognized by four types of receptors associated with innate immunity: Toll-like

receptors (TLRs), Nod-like receptors, retinoic acid-inducible gene-I (RIG-I) -like receptors and C-type lectins [1]. The initial recognition of pathogens by these receptors induces inflammatory reactions at the infected site, and also triggers adaptive immunity against the pathogens. Thus, activation of the innate immune response exerts antiviral effects. Immunity-associated receptor agonists are therefore good candidates for antiviral drugs and adjuvants [2].

IFN-α and IFN-β are currently employed therapeutically. The most noteworthy example is in the treatment of chronic hepatitis C virus (HCV) infection with pegylated IFN-α (PegIFN-α) [3]. These IFNs also are used against chronic hepatitis B virus (HBV) infection [4]. Some groups recently have reported that HCV infection results in expression of IFN-λs in primary human hepatocytes [5] and in the livers of chimpanzees [6]. Additionally, variation near the IFN-λ3 (IL-28B) -encoding gene is strongly associated with treatment response to pegylated IFN and ribavirin for chronic HCV infection and spontaneous eradication [7,8,9,10].

To target induction of the innate immune system of liver without inducing systemic immune activation, we developed a complex of cationic liposome (LIC) and the synthetic double-stranded RNA analog (polyinosinic-polycytidylic acid; pIC), termed LIC-pIC. We have reported that LIC is a safe and effective delivery tool for oligonucleotides [11,12]. Furthermore, we have shown, using administration in animal models, that RNA complexed with LIC can be delivered in large quantities to the liver (**Figure S1**). pIC is a well-known inducer of IFN-α and IFN-β production, a role mediated through pIC's recognition by TLR3 [13] or RIG-I-like receptors [14].

In the present study, we demonstrate, using administration of LIC-pIC, the distinct innate immune responses of human and mouse hepatocytes in chimeric mice harboring human/mouse livers infected with HCV or HBV [15,16]. The animals used here were transgenic severe combined immunodeficient (SCID) mice that carried additional copies of the urokinase plasminogen activator-encoding gene, resulting in the apoptosis of endogenous mouse hepatocytes, which then were replaced with human hepatocytes. This animal model provided robust HBV or HCV infection in chimeric mice harboring humanized livers. Because these rodents were T- and B-cell deficient, the mice were not appropriate for studies of adaptive immunity. Nonetheless, this model provided new insights into HCV innate host responses and therapeutic approaches. Furthermore, these models permitted analyses of human/mouse hepatocyte immune responses in the same liver. These analyses indicated that IFN-λs play a critical role in the antiviral response of human hepatocytes, and that IFN-β is induced in the response of mouse hepatocytes. Analysis of several cell lines showed that this robust IFN-λ induction was limited to the human hepatocytes. These results suggest that the function of IFN-λs, IFN-α, and IFN-β differ depending on the animal species and on the tissue under study.

Materials and Methods

Ethics Statement

This study was carried out in strict accordance with both the *Guidelines for Animal Experimentation* of the Japanese Association for Laboratory Animal Science and the recommendations in the *Guide for the Care and Use of Laboratory Animals* of the National Institutes of Health. All protocols were approved by the ethics committee of Tokyo Metropolitan Institute of Medical Science. The HCV-infected patient who served as the source of the serum samples provided written informed consent prior to blood collection.

Nucleic Acids and Complexes

pIC and LIC were prepared as previously described [11]. In brief, the distribution of the chain lengths of polyinosinic and polycytidylic acids (Yamasa, Chiba, Japan) was adjusted by heating to give an apparent maximum of 200–400 bases, as determined by gel filtration high-performance liquid chromatography. Liposomes composed of the cationic lipid analogue 2-*O*-(2-diethylaminoethyl)-carbamoyl-1,3-*O*-dioleoylglycerol (synthesized at Nippon Shinyaku Co., Ltd., Kyoto, Japan) and egg phosphatidylcholine (NOF Corp., Tokyo, Japan) were lyophilized and formulated by Nippon Shinyaku Co., Ltd. A short dsRNA, a synthetic siRNA against the firefly luciferase gene, was purchased from Hokkaido System Science (Sapporo, Japan). The sequence of this dsRNA was 5′-GCUAUGAAAC-GAUAUGGGC-dTdT-3′ (sense) and 5′-GCCCAUAUCGUUU-CAUAGC-dTdT-3′ (antisense). Atelocollagen, a highly purified type I collagen prepared by pepsin treatment of calf dermis, was obtained from Koken (Tokyo, Japan). Each nucleic acid complex with LIC or atelocollagen was freshly prepared for each experiment.

Generation of Chimeric Mice Infected with HCV or HBV

Chimeric mice infected with HCV or HBV were prepared as previously described [17,18]. In brief, uPA$^{+/+}$/SCID mice transplanted with human hepatocytes were obtained from PhoenixBio (Hiroshima, Japan) [19]. Six weeks after transplantation, we injected each chimeric mouse intravenously (IV) with HCV (10^6 copies per dose) -containing serum or HBV-containing culture supernatant. The serum was obtained from a HCV-infected patient harboring HCV genotype 1b (HCR6; accession number AY045702) or 1a (HCG9; accession number AB520610); the supernatant was concentrated from a culture containing HBV genotype C. By the time of the first drug administration, the serum HCV genomic RNA levels had reached 6.6×10^5 to 2.7×10^7 copies/ml (genotype 1b) or 2.9×10^6 to 2.8×10^8 copies/ml (genotype 1a); the serum HBV genomic DNA levels had reached 2.4×10^7 to 1.2×10^9 copies/ml.

Treatment of Chimeric Mice

Virus-infected chimeric mice with humanized livers were randomly allocated to treatment groups of 3–5 mice each. Starting on Day 0, the chimeras received once- or three-times-daily IV injections (via the tail or orbital vein) of saline, LIC-pIC, atelocollagen-pIC, LIC-short dsRNA, pIC, human IFN-λ1, human IFN-λ2, or human IFN-λ3 (the human IFN-λs were from R&D Systems, Minneapolis, MN, USA) and once-weekly (Days 0 and 7) IV injections of α-galactosylceramide (KRN7000; Kirin Brewery, Gunma, Japan); twice-weekly (Days 0, 3, 7 and 10) subcutaneous (SC) injections of 30 μg/kg PegIFN-α (PegIFNα-2a; Chugai Pharmaceutical Co., Ltd, Tokyo, Japan); or once-daily peroral entecavir (ETV) (Bristol-Myers Squibb, New York, NY, USA). The IV injections were performed under gentle pressure to avoid non-specific delivery effects. All drugs were administered at a dosing volume of 5–10 μl/g of body weight.

Quantification of HCV Genomic RNA Levels by qRT-PCR

Total RNA was purified from the serum or liver tissue of chimeric mice with humanized livers by the acid guanidinium-phenol-chloroform method. HCV genomic RNA levels were quantified by qRT-PCR with an ABI7700 sequence detector system (Applied Biosystems, Foster City, CA, USA) as previously described [20].

Quantification of HBV Genomic DNA by qPCR

DNA extraction from the serum and liver tissue, and quantification of HBV genomic DNA, were performed as previously described [21].

Immunofluorescence Analysis

Liver tissues obtained from mice were embedded in OCT compound. The frozen tissues were cut into thin sections (5–8 μm) and placed on glass slides. After fixation, mouse liver sections were probed with an anti-HCV core protein monoclonal antibody (5E3) labeled with biotin [22] as the primary antibody, followed by streptavidin Alexa-488 conjugate (Invitrogen Corp., Carlsbad, CA, USA). To detect human hepatocytes, liver sections were probed with anti-human hepatocyte monoclonal antibody (Dako, Glostrup, Denmark), followed by anti-mouse IgG-Alexa 546 (Molecular Probes). The nuclei were stained with 4′,6-diamidino-2-phenylindole (DAPI).

Cells

HepG2, Huh-7, and HEK293T cells were obtained from the American Type Culture Collection. MRC-5 (RCB0218) cells were provided by the RIKEN BioResource Center through the National Bio-Resource Project of the MEXT, Japan. All cells were cultured as described [23]. Two types of human hepatoma HuH-7 cells carrying an HCV sub-genomic replicon (FLR 3-1 (genotype 1b, Con-1) and R6FLR-N (genotype 1b, strain HCR6 and N)) were used and cultured as described [24], [25].

RNA-mediated Interference

Chemically synthesized 21-nucleotide siRNA, including control siRNA (siPerfect Negative control), was obtained from Sigma. The sequences of these RNAs are 5′-GCCAUAGACCACUCAGCUU-3′ (siTICAM-1) and 5′-CCACCUUGAUGCCUGUGAA-3′ (siMAVS) (only the sense strands are shown). Cells were transfected with 50 nM siRNA in 2.0 μl Lipofectamine RNAiMAX (Invitrogen), and then were used 48 h later for further experiments.

Microarray Analysis

Total RNA was extracted from chimeric mouse livers using ISOGEN (Nippon Gene, Tokyo, Japan), and was purified using an RNeasy Mini Kit (QIAGEN, Valencia, CA, USA). RNA integrity was assessed with a Bioanalyzer (Agilent Technologies, Santa Clara, CA, USA). cRNA was prepared and the microarray (Agilent Technologies) was hybridized and scanned according to the manufacturer's instructions. Whole human genome 4×44 K format microarrays (G4112F; Agilent Technologies) were used.

Gene Expression Analysis

Total RNA or cDNA, which was synthesized from total RNA using a High Capacity cDNA Reverse Transcription Kit (Applied Biosystems), was used for qRT-PCR or qPCR performed using TaqMan Gene Expression Assays and the ABI7700 sequence detector system. The TaqMan Gene Expression Assays for *IFNB1*, *Ifnb1*, *IFNA2*, *Ifna2*, *IFNG*, *Ifng*, *IFNL1* (also known as *IL29*), *Ifnl2/3* (also known as *Il28a/b*), *IFNAR1*, *Ifnar1*, *IFNAR2*, *Ifnar2*, *IFNLR1* (also known as *IL28RA*), and *Ifnlr1* (also known as *Il28ra*) were obtained from Applied Biosystems. The primers and probes for the *IFNL2* and *IFNL3* (also known as *IL28A* and *IL28B*, respectively) genes were obtained from Takara Bio, Inc. (Shiga, Japan). The primers and probes for the *IFNL2* gene consisted of a forward primer, IL28A-207-S21 (nt 207–227; 5′-GCTGAAGGACTGCAGGTGCCA-3′); a reverse primer, IL28A-378-R20 (nt 359–378; 5′-GGGCTGGTCCAAGACGTCCA-3′); and a TaqMan probe, IL28A-286-S24FT (nt 286–309; 5′-ATGGCTTTGGAGGCTGAGCTGGCC-3′). The primers and probes for the *IFNL3* gene consisted of a forward primer, IL28B-207-S21 (nt 207–227; 5′-GCTGAAGGACTGCAAGTGCCG-3′); a reverse primer, IL28B-379-R21 (nt 359–379; 5′-GGGGCTGGTCCAAGACATCCC-3′); and a TaqMan probe, IL28B-286-R20FT (nt 267–286; 5′-CGGGGCGCTCCCTCACCTGC-3′). A reporter dye, 6-carboxy-fluorescein, was covalently attached to the 5′-end of the probe sequence and a quencher dye, 6-carboxytetramethylrhodamine, was attached to its 3′-end.

Calibration curves for quantification of the IFN-α- or IFN-β-encoding genes and the IFN-λs-encoding genes were prepared by using a series of ten-fold dilutions of human *IFNB1* and *IFNA2* RNAs (synthesized in our laboratory), and human *IFNL1*, *IFNL2*, and *IFNL3* cDNA clones (Open Biosystems, Inc., Huntsville, AL, USA). Each assay specifically detected its own target.

Quantification of *IFNAR1/2*, *Ifnar1/2*, *IFNLR1*, and *Ifnlr1* mRNA was estimated using the calibration curves for the *IFNL1* cDNA.

IFN-λ Neutralization Studies

IFN-λ1 to IFN-λ3 in the chimeric mice were neutralized by daily IV injection of 3 mg/kg anti-human IFN-λ1 (R&D Systems) and 1 mg/kg anti-human IFN-λ2 (R&D Systems) antibodies.

Statistical Analysis

The data were analyzed with SAS System version 8.2 (SAS Institute, Inc., Cary, NC, USA). P values of ≤ 0.05 were considered significant.

Results

Antiviral Responses Elicited by LIC-pIC in HCV- or HBV-infected Chimeric Mice with Humanized Livers

To confirm that HCV and HBV can infect humanized chimeric mice, we measured HCV RNA or HBV DNA levels in serum weekly after inoculation with the respective virus (**Figure S2A and S2B**). At 3 weeks post-infection, HCV-RNA levels reached 10^6–10^7 copies/mL in the genotype 1b group (**Figure S2A**); at 9 weeks post-infection, HBV-DNA levels reached 10^7–10^8 copies/mL (**Figure S2B**). These results demonstrated that HCV or HBV can replicate in, and persistently infect, human hepatocytes transplanted into chimeric mice.

Treatment of HCV genotype 1b-infected chimeric mice with LIC-pIC (0.1 mg/kg; 1 or 3 times/day) led to a dose-dependent reduction in serum HCV RNA that was greater than the reduction induced by PegIFN-α treatment (30 μg/kg; twice/week, 20-fold the typical clinical dose) (**Figure 1A**). Treatment of HCV genotype 1a-infected mice with LIC-pIC (0.01, 0.03 or 0.1 mg/kg; once/day) had a similar antiviral effect (**Figure 1B**). Treatment of these mice with LIC-pIC also reduced liver HCV RNA levels (**Figure 1C**) and liver HCV core protein levels (**Figure 1D**).

Treatment with LIC-pIC (0.1 mg/kg/day) also reduced serum HBV DNA levels in HBV-infected mice more effectively than entecavir (ETV) treatment (17 μg/kg/day; the same as the clinical dose) by Day 14 (**Figure 1E**) and additionally reduced liver HBV DNA levels (**Figure 1F**). LIC-pIC complex treatment therefore elicited stronger antiviral responses against both HCV and HBV than currently used antiviral agents without marked hepatotoxicity (**Figure S3**).

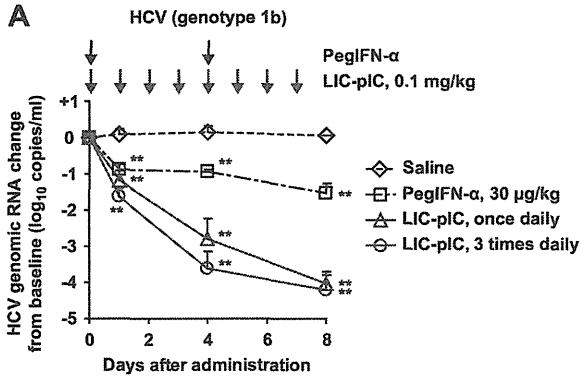
A
HCV (genotype 1b)
PegIFN-α
LIC-pIC, 0.1 mg/kg
HCV genomic RNA change from baseline (log10 copies/ml)
Days after administration
Saline
PegIFN-α, 30 μg/kg
LIC-pIC, once daily
LIC-pIC, 3 times daily

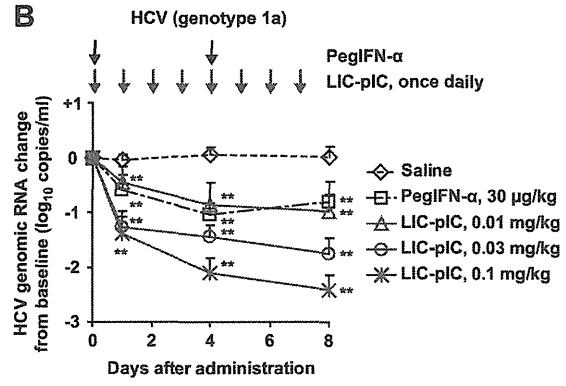
B
HCV (genotype 1a)
PegIFN-α
LIC-pIC, once daily
HCV genomic RNA change from baseline (log10 copies/ml)
Days after administration
Saline
PegIFN-α, 30 μg/kg
LIC-pIC, 0.01 mg/kg
LIC-pIC, 0.03 mg/kg
LIC-pIC, 0.1 mg/kg

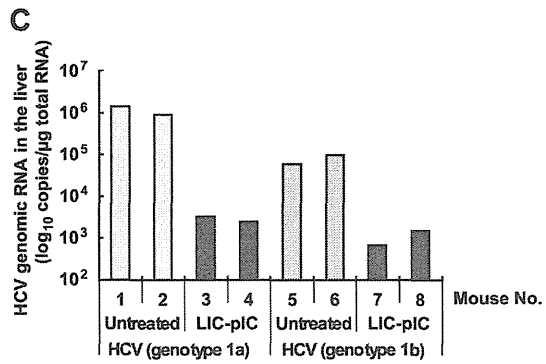
C
HCV genomic RNA in the liver (log10 copies/μg total RNA)
Mouse No.
Untreated
LIC-pIC
Untreated
LIC-pIC
HCV (genotype 1a)
HCV (genotype 1b)

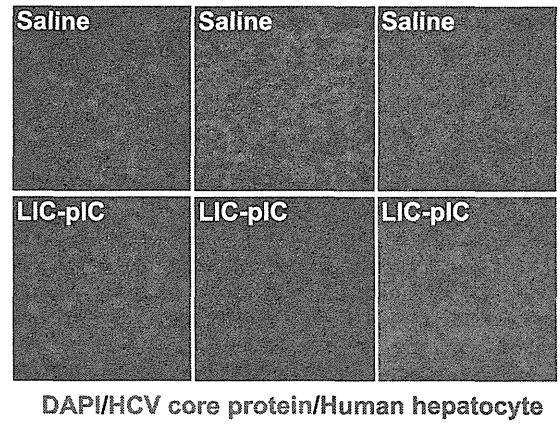
D
Saline
Saline
Saline
LIC-pIC
LIC-pIC
LIC-pIC
DAPI/HCV core protein/Human hepatocyte

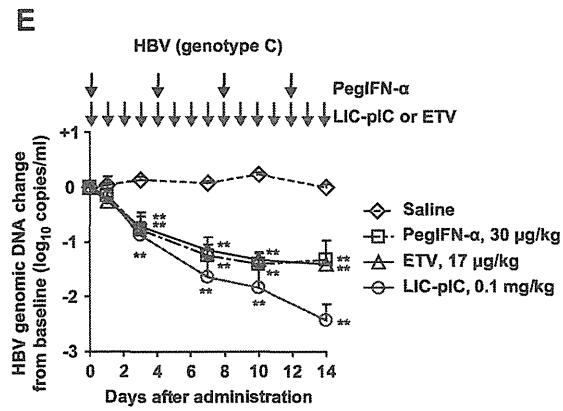
E
HBV (genotype C)
PegIFN-α
LIC-pIC or ETV
HBV genomic DNA change from baseline (log10 copies/ml)
Days after administration
Saline
PegIFN-α, 30 μg/kg
ETV, 17 μg/kg
LIC-pIC, 0.1 mg/kg

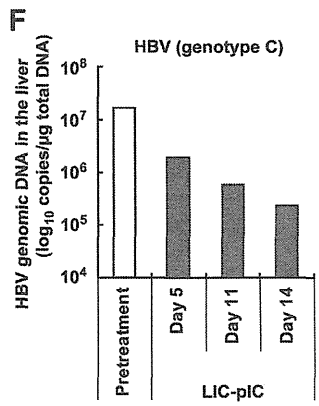
F
HBV (genotype C)
HBV genomic DNA in the liver (log10 copies/μg total DNA)
Pretreatment
Day 5
Day 11
Day 14
LIC-pIC

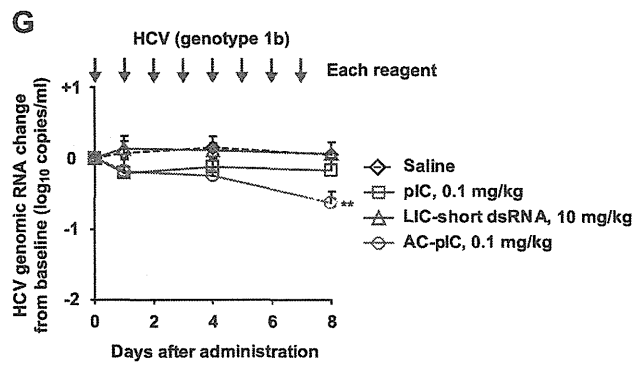
G
HCV (genotype 1b)
Each reagent
HCV genomic RNA change from baseline (log10 copies/ml)
Days after administration
Saline
pIC, 0.1 mg/kg
LIC-short dsRNA, 10 mg/kg
AC-pIC, 0.1 mg/kg

Figure 1. Antiviral responses elicited by LIC-pIC in chimeric mice with humanized livers. (**A**, **B**) Serum HCV RNA levels, relative to the baseline, in HCV genotype 1b-infected (**A**) or 1a-infected (**B**) chimeric mice following the indicated treatments, as determined by qRT-PCR ($n = 3$–5 per group). (**C**) Liver HCV RNA levels on Day 4 of LIC-pIC treatment (0.1 mg/kg/day), as determined by qRT-PCR. (**D**) Immunostained liver tissues of HCV genotype 1b-infected chimeric mice treated with saline (Upper) and LIC-pIC (0.1 mg/kg/day) (Lower) at Day 4. (**E**) Serum HBV DNA levels relative to the baseline following the indicated treatments, as determined by qPCR ($n = 3$–4 per group). (**F**) HBV DNA levels of chimeric mouse livers following LIC-pIC treatment, as determined by qPCR ($n = 1$ per each time point, the results indicates the mean of two measurements) (**G**) HCV RNA levels relative to the baseline following the indicated treatments, as determined by qRT-PCR ($n = 3$–4 per group). In all cases, bars indicate SD. $^{**}P<0.01$, treatment vs. saline control by Dunnett's multiple comparison test.
doi:10.1371/journal.pone.0059611.g001

We next analyzed the effect on serum HCV RNA levels of treatment with pIC alone; with pIC complexed with the non-hepatotropic carrier atelocollagen (AC) [26]; or with a short dsRNA complexed with LIC. Significant reductions in serum HCV RNA levels were observed only following treatment with the AC-pIC complex (**Figure 1G**), indicating that the active ingredient of LIC-pIC was pIC and that the antiviral effects of pIC were enhanced by complexing with LIC.

Expression of IFN-α, IFN-β and IFN-γ Induced by LIC-pIC in Chimeric Mice with Humanized Livers

pIC induces IFN-α and IFN-β production through recognition by TLR3 [13] or RIG-I-like receptors [14]. To examine whether the potent antiviral responses elicited by LIC-pIC were caused by its reported ability to induce IFN-α and IFN-β, we analyzed the expression levels of these IFNs after administration of 0.1 mg/kg LIC-pIC to virally infected mice. Administration and sampling were conducted according to the schedules shown in **Figure 2A** (HCV-infected mice) and **Figure S4A** (HBV-infected mice). Because the mouse livers used in this study were human-mouse chimeras (average substitution rate ≈80%) [19], we measured the induction levels of both human and mouse IFNs.

The first administration of LIC-pIC (Day 0) induced both human and mouse IFN-β in the serum, as well as *IFNB1* (human) and *Ifnb1* (mouse) mRNA in the liver (**Figure 2B and 2C**). The mRNA induction levels peaked 3 h after the first administration and decreased to the pretreatment levels within 24 h (data not shown). On repeated administration, the peak levels of both protein and mRNA fell gradually in the mouse, whereas induction of humanized liver-derived IFN products was observed only at the first administration (**Figure 2B and 2C**), although the antiviral responses elicited by LIC-pIC were sustained throughout the administration period. In addition, we did not observe induction of human or mouse IFN-α in the serum, or of *IFNA2* or *IFNG* (human) or *Ifna2* or *Ifng* (mouse) mRNA in the liver, at any point during LIC-pIC administration (**Figure 2B and 2C**, and **Figure S4B** and **S4C**). The induced mouse IFN-β that was still observed after the fifth administration was not expected to have any antiviral effect because mouse IFN-β does not suppress HCV replication in HCV replicon-containing cells (**Figure 2D**), indicating that mouse IFN-β does not activate signaling by the human receptor. Thus, the kinetics of IFN-α, IFN-β, and IFN-γ induction by LIC-pIC were inconsistent with the duration of the antiviral responses that were observed.

Moreover, the maximum serum concentration of human IFN-β that was induced by LIC-pIC was only 92 pg/ml (**Figure 2B**), which was 13-fold lower than the serum level of mouse IFN-β, despite the high human hepatocyte substitution rate in the liver. This poor induction of human IFN-β by LIC-pIC was independent of HCV infection (**Figure S5**). As for IFN-α, no serum IFN-α could be detected following LIC-pIC treatment, whereas a constant high concentration of human IFN-α (≈20,000 pg/ml) was observed in the serum of chimeric mice treated with PegIFN-α (**Figure 2B**). Thus, the concentration of IFN-α and IFN-β in the serum of chimeric mice treated with LIC-pIC could not explain the potency of the LIC-pIC-induced antiviral response.

Although pIC is also known as an activator of natural killer (NK) or NKT cells [27,28], these cell types were not involved in the antiviral response elicited by LIC-pIC in the virus-infected chimeric mice of this study (**Figure S6**). These cumulative data indicated that an unknown mechanism was responsible for the observed antiviral response.

IFN-λs Mediate the Antiviral Response of Chimeric Mice with Humanized Livers to LIC-pIC

To determine the mechanism of the LIC-pIC-induced antiviral response, we performed comprehensive gene expression analysis to identify genes whose expression kinetics were consistent with the duration of this response. DNA microarray analysis of the livers of chimeric mice infected with HCV and treated, or not, with LIC-pIC identified type III IFN genes as having suitable expression kinetics (**Figure 3A and 3B**). There are three type III IFN genes in humans, *IFNL1*, *IFNL2*, and *IFNL3* (formerly *IL29*, *IL28A*, and *IL28B*, respectively), which encode IFN-λ1, IFN-λ2 and IFN-λ3 (also designated IL-29, IL-28A, and IL-28B), respectively [29,30]. The genes that were analyzed included those encoding IFN-α, IFN-β, IFN-ε, IFN-κ, IFN-ω, IFN-γ, and IFN-λ. Among these genes, the three IFN-λ-encoding genes were the only ones whose levels remained up-regulated 3 h after the fifth LIC-pIC administration to HCV-infected mice on Day 4 (**Figure 3B**). qRT-PCR demonstrated that, unlike *IFNB1*, the mRNA levels of human *IFNL1* (*IL29*), *IFNL2* (*IL28A*), and *IFNL3* (*IL28B*) were strongly induced in the livers of chimeric mice treated with LIC-pIC (**Figure 3C**). In addition, expression of human *IFNL1*, *IFNL2*, and *IFNL3* was induced at each LIC-pIC administration. Consistent with these gene expression results, ELISA analysis revealed that the serum levels of IFN-λ1 and IFN-λ2 were much higher than the level of IFN-β (**Figure 3D**). These results indicated that the expression of IFN-λs was strongly and persistently induced by LIC-pIC in human hepatocytes transplanted into chimeric mice.

We further investigated whether IFN-λs directly affected HCV or HBV replication. Indeed, recombinant human IFN-λ1, IFN-λ2, and IFN-λ3, when added to HCV replicon cells, suppressed virus replication in a concentration-dependent manner (**Figure S7**). Furthermore, chimeric mice dosed with IFN-λs had (by Day 8) serum HCV RNA levels that were significantly lower than those of the saline-treated control group (**Figure 3E**). Treatment with IFN-λ2 also reduced serum HBV DNA levels compared to those seen in the saline-treated control group by Day 7 (**Figure S8**). Furthermore, combination treatments with neutralizing antibodies against IFN-λ1 and IFN-λ2 (a treatment that neutralizes all three IFN-λ subtypes due to cross-reactivity (**Figure S9**)) attenuated the LIC-pIC-dependent reduction in HCV RNA levels in both serum and liver (**Figure 3F**). These results demonstrated that IFN-λs play a critical role in the antiviral response elicited in human hepatocytes by LIC-pIC.

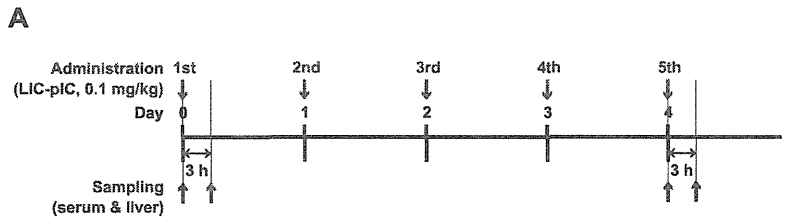
A
Administration (LIC-pIC, 0.1 mg/kg)
1st
2nd
3rd
4th
5th
Day
0
1
2
3
4
3 h
3 h
Sampling (serum & liver)

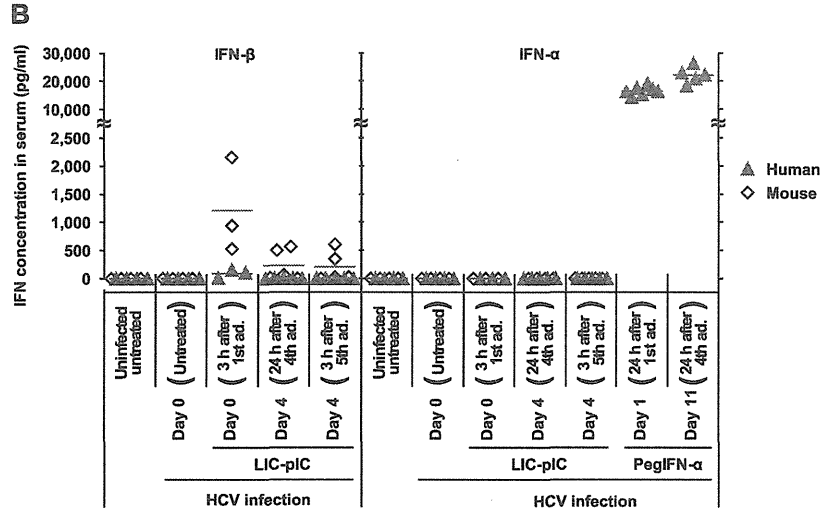
B
IFN concentration in serum (pg/ml)
IFN-β
IFN-α
Human
Mouse
Uninfected untreated
Untreated
3 h after 1st ad.
24 h after 4th ad.
3 h after 5th ad.
Day 0
Day 4
Day 1
Day 11
LIC-pIC
PegIFN-α
HCV infection

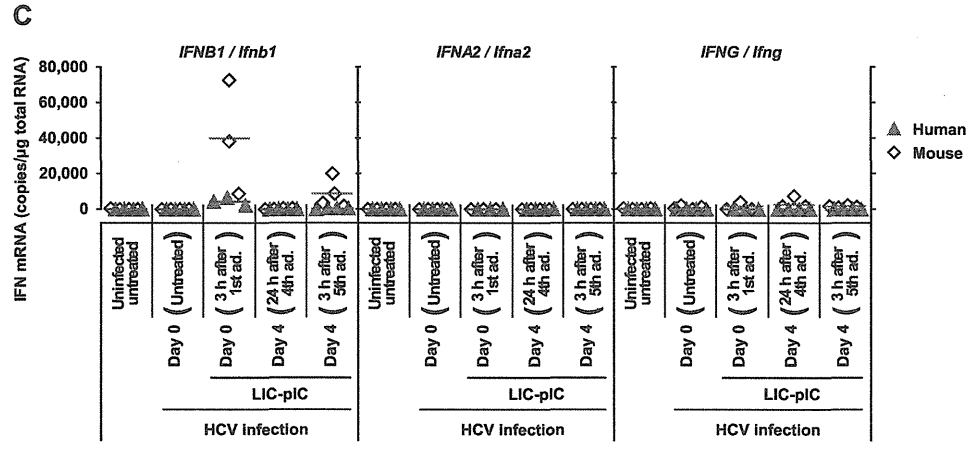
C
IFN mRNA (copies/μg total RNA)
IFNB1 / Ifnb1
IFNA2 / Ifna2
IFNG / Ifng
Human
Mouse
Uninfected untreated
Untreated
3 h after 1st ad.
24 h after 4th ad.
3 h after 5th ad.
Day 0
Day 4
LIC-pIC
HCV infection

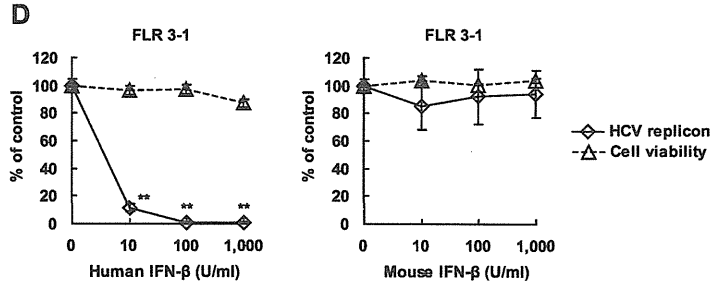
D
FLR 3-1
FLR 3-1
% of control
HCV replicon
Cell viability
Human IFN-β (U/ml)
Mouse IFN-β (U/ml)

Figure 2. Expression of genes encoding IFN-α, IFN-β, and IFN-γ following induction by LIC-pIC in chimeric mice with humanized livers. (**A**) Experimental schedule in chimeric mice infected with HCV. (**B**) Serum concentrations (in chimeric mice) of human and mouse IFN-β and IFN-α, as determined by ELISA ($n=3$–5 for no treatment or LIC-pIC group; $n=6$–8 for PegIFN-α group). Bars indicate the mean concentration of human (red) and mouse (green) IFNs averaged across the entire group. The results indicates the representative of two measurements (**C**) The liver mRNA levels of genes encoding IFN-β, IFN-α2 and IFN-γ (human genes: *IFNB1, IFNA2* and *IFNG*, respectively; mouse genes: *Ifnb1, Ifna2* and *Ifng*, respectively), as determined by qRT-PCR ($n=3$–4 per group). The bars indicate the mean mRNA levels of human (red) and mouse (green) IFN genes averaged across the entire group. The results indicates the representative of two measurements (**D**) Effectiveness of recombinant human or mouse IFN-β against HCV in FLR 3-1 HCV-replicon cells. The bars indicate SD ($n=4$ per group). $^{**}P<0.01$, treatments vs. the vehicle by Dunnett's multiple comparison test.
doi:10.1371/journal.pone.0059611.g002

The Induction of IFN-λs by LIC-pIC and Antiviral Effect in Humanized Chimeric Mice with Genetic Variants of IFNL3 (IL28B)

Patients with the G-allele of rs8099917, a SNP that is located near the *IFNL3* gene, are less likely to spontaneously clear acute HCV infection and respond to combination therapy with PegIFN-α and ribavirin [7,8,9,10]. We examined whether this genetic variation influenced the induction of IFN-λs in human hepatocytes and antiviral response to HCV. In the present study, LIC-pIC induced IFN-λ gene expression and anti-HCV effects to the same degree, even in chimeric mice harboring human hepatocytes derived from donors bearing the rs8099917 G-allele (**Figure S10A** and **10B**). These results indicate that neither induction of IFN-λs by LIC-pIC nor antiviral response was significantly influenced by this genomic polymorphism.

The Difference in Innate Immunity Induced by LIC-pIC in Human and Mouse Livers

The present study used chimeric mice with humanized livers, a model that permitted simultaneous analysis of human and mouse gene expression in the same liver. With LIC-pIC treatment, expression of IFN-λ-encoding genes was induced to levels greater than those of IFN-α- and IFN-β-encoding genes in human hepatocytes, whereas *Infb1* was induced to levels greater than expressions of IFN-λ-encoding genes in mouse hepatocytes (**Figure S11A**). Moreover, gene expression analysis indicated that the expression patterns of the genes encoding the corresponding IFN receptors differed between the human and mouse hepatocytes. Specifically, the genes encoding the IFN-α and IFN-β receptors were more strongly expressed in mouse hepatocytes (as *Ifnar1* and *Ifnar2*, respectively) than in human hepatocytes (as *IFNAR1* and *IFNAR2*, respectively), whereas the gene encoding the IFN-λ receptor was more strongly expressed in human hepatocytes (as *IFNLR1* (formerly *IL28RA*)) than in mouse hepatocytes (as *Ifnlr1* (formerly *Il28ra*)) (**Figure S11B**, **S11C**, and **S11D**). These results strongly suggest that IFN-λs play a critical role in the immune response by human hepatocytes, while IFN-α and IFN-β are important for the response by mouse hepatocytes.

IFN Expression in Human Cell Lines Following the Induction of Innate Immunity with Various Stimuli

To provide a comparison with the innate immune response of human hepatocytes, we investigated the role of IFNs in cell lines derived from other tissues. For this purpose, we examined the expression levels of the genes encoding IFN-λ and IFN-β following treatment with LIC-pIC in several human cell lines. In response to treatment with LIC-pIC, *IFNL1* mRNA was more strongly induced in HepG2 cells, a hepatocyte cell line, than in HEK293T or MRC-5 cells, kidney and fibroblast cell lines, respectively; the opposite expression pattern was observed for the induction of *IFNB1* mRNA (**Figure 4A**). Indeed, the protein level of IFN-λ1 in cell culture medium was also much higher in HepG2 cells than in MRC-5 cells (**Figure 4B**). Interestingly, whereas LIC-pIC induction of *IFNL1* mRNA and IFN-λ1 protein was weaker in MRC-5 cells than in HepG2 cells, the levels of *IFNL1* mRNA and IFN-λ1 protein in MRC-5 cells were almost comparable to those seen in HepG2 cells upon infection with Newcastle disease virus (NDV) or vesicular stomatitis virus (VSV) (**Figure 4C and 4D**). These data suggest that the *IFNL1*/IFN-λ1 expression profile induced by LIC-pIC was different from that induced upon viral infection. Using siRNA technology, we found that the expression of *IFNL1* induced by LIC-pIC was mediated by both MAVS (the adaptor molecule that links RIG-I-like receptor signaling pathways) and TICAM-1 (a TLR adaptor molecule) (**Figure 4E and 4F**). These results suggest that the innate immune response of human hepatocytes has unique characteristics in terms of IFN responses, and that LIC-pIC can induce robust production of IFN-λs by human hepatocytes through recognition by two distinct innate immune molecules (**Figure 4G**).

Discussion

In this study, we demonstrated that treatment of chimeric mice (harboring human hepatocytes) with LIC-pIC resulted in the efficient induction of innate immunity that was associated with robust production of IFN-λs and resulted in the abrogation of infection by hepatotropic viruses such as HCV and HBV. Recently, two different groups, Marukian *et al.* [5] and Thomas *et al.* [6], have reported that HCV infection results in production of IFN-λs in primary human hepatocytes and in the livers of chimpanzees, providing control of HCV replication. In the present study, we extend those analyses by showing that the activation of the intrinsic immune system in human hepatocytes induces the robust production of IFN-λs, thereby providing efficient defense against viral pathogens. Furthermore, we show that neither induction of IFN-λs by LIC-pIC nor associated antiviral effects are influenced significantly by a genomic polymorphism near the *IFNL3* gene. In contrast, the efficacy of combination therapy of PegIFN-α and ribavirin varies with genomic variations at this site. More recently, Prokunina-Olsson *et al.* have demonstrated that a dinucleotide variant, ss469415590 (TT or ΔG), located upstream of *IFNL3* is strongly associated with HCV clearance, and that its frameshift variant ss469415590[ΔG] creates a new gene, termed *IFNL4* [31]. These findings may provide a new approach to investigate whether treatment with LIC-pIC induces *IFNL4* and whether the antiviral effects of LIC-pIC are influenced by the induction of *IFNL4*.

To date, several mouse studies have indicated that IFN-λs play an important role in host defense against pathogens in vaginal, intestinal, and tracheal epithelial cells [32,33,34], but that these IFN molecules do not contribute to innate immunity against hepatotropic viruses [35]. In the present study, we showed that LIC-pIC treatment activated the innate immune response of human hepatocytes in chimeric mouse liver, providing robust expression of the IFN-λ-encoding gene without significantly inducing expression of the IFN-β-encoding gene. Moreover, we showed that human hepatocytes expressed the IFN-λ receptor-

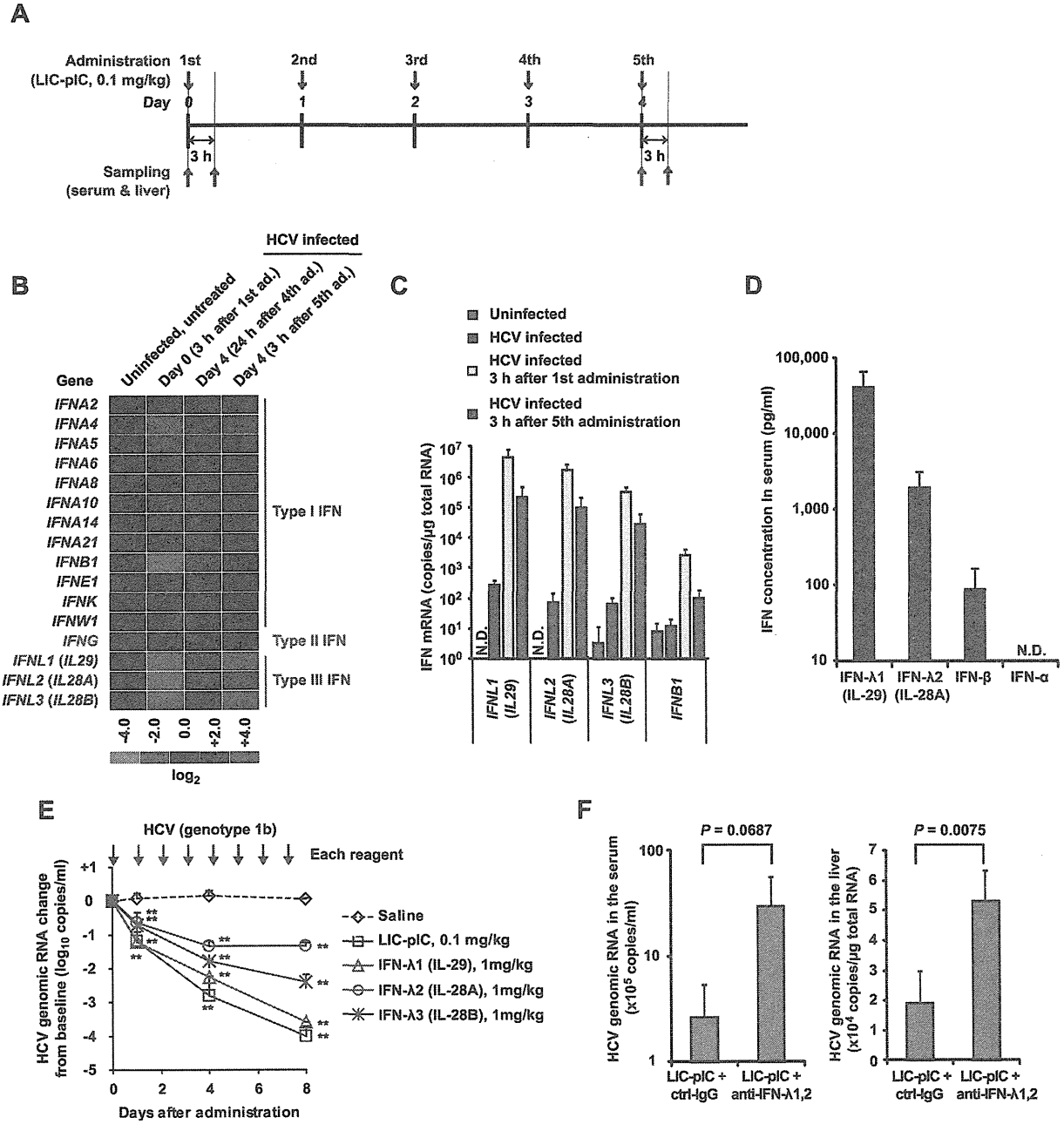

Figure 3. IFN expression following induction of innate immunity by LIC-pIC. (**A**) Experimental schedule in the chimeric mice infected with HCV. (**B**) Microarray analysis of IFN family gene expression. Log_2 ratio values of gene expression were calculated with respect to control (untreated and HCV-infected) chimeric mice. (**C**) Liver mRNA levels of human IFN genes ($n = 3$–5 per group), as determined by qRT-PCR. (**D**) Serum concentration of human IFN-λ1, IFN-λ2, IFN-β, and IFN-α ($n = 3$ per group), as determined by ELISA. (**E**) Serum HCV RNA levels, relative to the baseline, in HCV-infected chimeric mice treated with human IFN-λ, LIC-pIC, or control saline ($n = 3$–5 per group), as determined by qRT-PCR. (**F**) The HCV RNA levels in the serum and liver of HCV genotype 1a-infected chimeric mice collected on Day 4 of LIC-pIC treatment, as determined by qRT-PCR. The mice were additionally treated with either a control antibody or a neutralizing antibody against IFN-λ ($n = 3$ per group). Bars indicate SD. $^{**}P<0.01$, treatments vs. saline controls on the respective day, by Dunnett's multiple comparison test.
doi:10.1371/journal.pone.0059611.g003

encoding genes at high levels, while expression of the IFN-β receptor-encoding genes remained low. In contrast, expression of the IFN-λ receptor-encoding genes was low and expression of the IFN-β receptor-encoding genes was high in mouse hepatocytes from the same livers. Thus, human hepatocytes (in contrast to mouse hepatocytes) are rich sources of IFN-λs, while IFN-α or IFN-β are produced at lower levels in these cells. Indeed, the expression (in humanized livers) of these IFN-λ-encoding genes

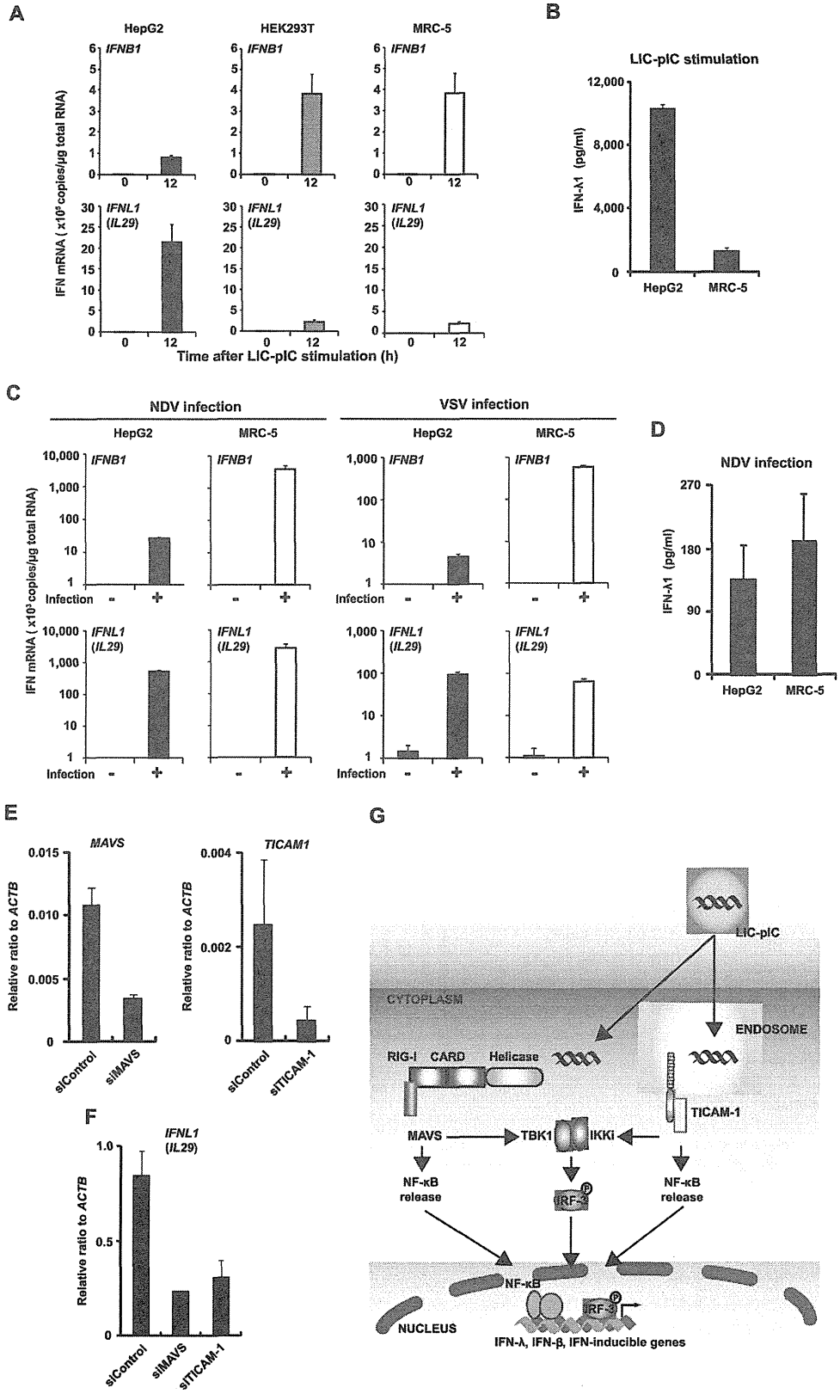
A
HepG2
HEK293T
MRC-5
IFNB1
IFNL1 (IL29)
IFN mRNA (x10³ copies/μg total RNA)
Time after LIC-pIC stimulation (h)
B
LIC-pIC stimulation
IFN-λ1 (pg/ml)
HepG2
MRC-5
C
NDV infection
VSV infection
Infection
D
NDV infection
E
MAVS
TICAM1
Relative ratio to ACTB
siControl
siMAVS
siTICAM-1
F
G
LIC-pIC
CYTOPLASM
ENDOSOME
RIG-I
CARD
Helicase
TICAM-1
MAVS
TBK1
IKKi
NF-κB release
IRF-3
NF-κB
NUCLEUS
IFN-λ, IFN-β, IFN-inducible genes